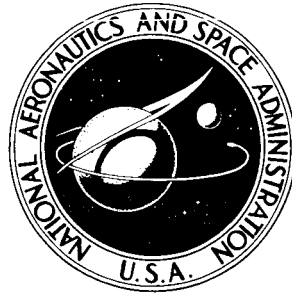


N 73-27544

**NASA CONTRACTOR
REPORT**



NASA CR-2289

NASA CR-2289

CASPER
COPY

**VARIATION OF THE LOW LEVEL WINDS
DURING THE PASSAGE OF
A THUNDERSTORM GUST FRONT**

by R. W. Sinclair, R. A. Anthes, and H. A. Panofsky

Prepared by

THE PENNSYLVANIA STATE UNIVERSITY

University Park, Pa. 16802

for George C. Marshall Space Flight Center

NATIONAL AERONAUTICS AND SPACE ADMINISTRATION • WASHINGTON, D. C. • JULY 1973

1. REPORT NO. NASA CR-2289		2. GOVERNMENT ACCESSION NO.		3. RECIPIENT'S CATALOG NO.	
4. TITLE AND SUBTITLE Variation of the Low Level Winds During the Passage of a Thunderstorm Gust Front				5. REPORT DATE July 1973	
				6. PERFORMING ORGANIZATION CODE M113	
7. AUTHOR(S) R. W. Sinclair, R. A. Anthes, and H. A. Panofsky				8. PERFORMING ORGANIZATION REPORT #	
9. PERFORMING ORGANIZATION NAME AND ADDRESS The Pennsylvania State University University Park, Pennsylvania 16802				10. WORK UNIT NO.	
				11. CONTRACT OR GRANT NO. NAS8-27334	
12. SPONSORING AGENCY NAME AND ADDRESS National Aeronautics and Space Administration Washington, D. C. 20546				13. TYPE OF REPORT & PERIOD COVERED Jan. 1972 - Nov. 1972 CONTRACTOR	
				14. SPONSORING AGENCY CODE	
15. SUPPLEMENTARY NOTES This report prepared under the technical monitorship of the Aerospace Environment Division, Aero-Astroynamics Laboratory, NASA-Marshall Space Flight Center.					
16. ABSTRACT Three time histories of wind profiles in thunderstorm gust fronts at Cape Kennedy and three at Oklahoma City are analyzed. Wind profiles at maximum wind strength below 100 m follow logarithmic laws, so that winds above the surface layer can be estimated from surface winds once the roughness length is known. A statistical analysis of 81 cases of surface winds during thunderstorms at Tampa revealed no predictor with skill to predict the time of maximum gust. Some 34% of the variance of the strength of the gust is accounted for by a stability index and surface wind prior to the gust; the regression equations for these variables are given. The coherence between microscale wind speed variations at the different levels has the same proportions as in non-thunderstorm cases.					
17. KEY WORDS thunderstorm front gusts aircraft response wind shear			18. DISTRIBUTION STATEMENT 20		
19. SECURITY CLASSIF. (of this report) unclassified	20. SECURITY CLASSIF. (of this page) unclassified	21. NO. OF PAGES 71	22. PRICE \$3.00		

FOREWORD

The research reported herein was supported by NASA Contract NAS8-27334. Dr. George H. Fichtl of the Aerospace Environment Division, Aero-Astroynamics Laboratory, Marshall Space Flight Center, was the scientific monitor, and support was provided by Mr. John Enders of the Aeronautical Operating Systems Division, Office of Advanced Research and Technology, NASA Headquarters.

The research reported in this document is concerned with the results of a study of the empirical characteristics of thunderstorm gust fronts for the design and safe operation of aeronautical systems. It is part of an investigation of the effect of severe atmospheric forcing on aeronautical systems. Portions of the study relating to vehicle response, numerical modeling of the gust front, and statistical analysis of evolutionary processes will be made available as they are completed.

The data used herein was supplied by NASA through Dr. Fichtl and the National Severe Storms Laboratory through Dr. Edwin Kessler. Mr. Dennis Deaven of the Department of Meteorology at Penn State provided invaluable aid with the computer analyses used herein.

TABLE OF CONTENTS

	<u>Page</u>
LIST OF TABLE	v
LIST OF FIGURES	vi
1.0 INTRODUCTION	1
1.1 Statement of Problem	1
1.2 Previous Reasearch	1
1.3 Specific Goal of This Research	6
2.0 THE OBSERVATIONS	7
2.1 Kennedy Tower Data	7
2.2 NSSL-WKY Tower Data	9
2.3 Tampa Data	9
3.0 ANALYSIS OF TOWER DATA	11
3.1 Relevant Time Scales	11
3.2 Smoothing the Wind Data	18
3.3 Summary of the Six Gust Front Cases	18
4.0 MODELING THE THUNDERSTORM GUST FRONT	24
4.1 Scaled Time-height Cross Sections	24
4.2 Test of Logarithmic Wind Law Hypothesis	28
4.3 Comparison of Roughness Length Under Thunderstorm Conditions with Those Under Non-thunderstorm Conditions	36
4.4 Implications of the Logarithmic Wind Law for the Prediction of the Gust Front Wind Speeds	38
5.0 STATISTICAL RELATIONSHIP OF GUST FRONT PARAMETERS TO RAWINSODE AND RADAR VARIABLES	50
5.1 Choice of Independent Variables	50
5.2 The Variation of Δt Based on a Simple Kinematic Model	51
5.3 Development of Regression Equations	56
5.4 Discussion of Regression Equations	59
REFERENCES	64

LIST OF TABLES

<u>Table</u>		<u>Page</u>
1	Values of descriptive parameters for the six gust fronts	23
2	Average wind directions, average ratio of 90 m winds to 18 m winds and corresponding roughness lengths for the six gust fronts. Also shown are previously determined roughness lengths for the listed wind directions	40
3	Means and standard deviations for each variable and correlation coefficients for each possible pair of variables for the 81 thunderstorm cases from Tampa, Florida	58

LIST OF FIGURES

<u>Figure</u>		<u>Page</u>
1	Time-height cross section of the one-second average wind speeds for the Florida gust front of July 27, 1967	8
2a	Time-height cross section of the 130-second running mean of wind speeds for the Florida gust front of July 27, 1967. The isotachs in this figure are expressed in mps	12
2b	Time-height cross section of the 130-second running mean of wind directions for the Florida gust front of July 27, 1967. The isogons in this figure are expressed in degrees	13
3a	Time-height cross section of the 130-second running mean of wind speeds for the Florida gust front of April 29, 1968. The isotachs in this figure are expressed in mps	14
3b	Time-height cross section of the 130-second running mean of wind directions for the Florida gust front of April 29, 1968. The isogons in this figure are expressed in degrees	15
4a	Time-height cross section of the 130-second running mean of wind speeds for the Florida gust front of June 25, 1968. The isotachs in this figure are expressed in mps	16
4b	Time-height cross section of the 130-second running mean of wind directions for the Florida gust front of June 25, 1968. The isogons in this figure are expressed in degrees.	17
5	Time-height cross section of the hand-smoothed wind speeds for the Oklahoma gust front of April 16, 1969. The isotachs in this figure are expressed in mps	19
6	Time-height cross section of the manually-smoothed wind speeds for the Oklahoma gust front of April 29, 1969. The isotachs in this figure are expressed in mps	20
7	Time-height cross section of the manually-smoothed wind speeds for the Oklahoma gust front of May 31, 1969. The isotachs in this figure are expressed in mps	21
8	Scaled time-height cross section of wind speed for the Florida gust front of July 27, 1967	25

LIST OF FIGURES (Continued)

<u>Figure</u>		<u>Page</u>
9	Scaled time-height cross section of wind speed for the Florida gust front of April 29, 1968	26
10	Scaled time-height cross section of wind speed for the Florida gust front of June 25, 1968	27
11	Ratio of wind speed to speed at 18 m vs. height and scaled time for the Florida gust front of July 27, 1967	30
12	Ratio of wind speed to speed at 18 m vs. height and scaled time for the Florida gust front of April 29, 1968	31
13	Ratio of wind speed to speed at 18 m vs. height and scaled time for the Florida gust front of June 25, 1968	32
14	Ratio of wind speed to speed at 18 m vs. height and scaled time for the Oklahoma gust front of April 16, 1969	33
15	Ratio of wind speed to speed at 18 m vs. height and scaled time for the Oklahoma gust front of April 26, 1969	34
16	Ratio of wind speed to speed at 18 m vs. height and scaled time for the Oklahoma gust front of May 31, 1969	35
17	Roughness length, z_o , as a function of direction at the Kennedy tower (Blackadar et al., 1972)	37
18	Roughness length, z_o , as a function of direction at the WKY Oklahoma tower	38
19	Comparison of observed 90 m wind with the 30 m wind multiplied by the average ratio, V_{90}/V_{30} , for the Florida gust front of July 27, 1967	42
20	Comparison of observed 90 m wind with the 30 m wind multiplied by the average ratio, V_{90}/V_{30} , for the Florida gust front of April 29, 1968	43

LIST OF FIGURES (Continued)

<u>Figure</u>		<u>Page</u>
21	Comparison of observed 90 m wind with the 30 m wind multiplied by the average ratio, V_{90}/V_{30} , for the Florida gust front of June 25, 1968	44
22	Comparison of observed 90 m wind with the 7 m wind multiplied by the average ratio, V_{90}/V_7 , for the Oklahoma gust front of April 16, 1969	45
23	Comparison of observed 90 m wind with the 7 m wind multiplied by the average ratio, V_{90}/V_7 , for the Oklahoma gust front of April 26, 1969	46
24	Comparison of observed 90 m wind with the 7 m wind multiplied by the average ratio, V_{90}/V_7 , for the Oklahoma gust front of May 31, 1969	47
25	Schematic diagram of gust front	52
26	Δt vs. gust front age	54
27	Δt vs. station distance from center of storm track (ℓ)	55
28	Scatter diagram with line of best fit of the speed maximum vs. the average speed before the gust front	60
29	Scatter diagram with line of best fit of the speed maximum vs. the instability index	62

1.0 INTRODUCTION

1.1 Statement of Problem

One atmospheric phenomenon that may adversely affect the operation of aeronautical systems is the cold surge or gust front accompanying thunderstorms. As the cold downdraft associated with the mature or decaying thunderstorm cell reaches the ground and spreads out horizontally, this cool, relatively dense air pushes under the warmer, lighter ambient air. The interface between the two air masses of different densities is called the pseudo cold front or gust front. This front may precede the main storm cell by as much as ten miles. The strong vertical and horizontal wind shears associated with the gusty winds behind the front are potential dangers to the safe operation of aircraft and launch vehicles.

In this report we investigate the structural properties of six gust fronts. Of particular interest is the variation of wind speed with time and height. In an effort to develop a statistical prediction scheme for the wind speed from the surface to about 150 m during the passage of a gust front, we have scaled the winds so that certain similarities among storms are present. We then attempt to relate the scaling parameters to measurable synoptic scale and radar variables, based on data from 81 thunderstorm cases in Tampa, Florida.

1.2 Previous Research

The low-level variation of wind under high wind conditions has been the subject of numerous empirical studies. As early as 1937, Sherlock and

Stout (1937) investigated the effect of wind loading of electric power lines during high wind situations. They analyzed the vertical variation (up to 250 feet) of wind during two winter storms, and noted that gust maxima occurred in the upper levels first: a time lag of several seconds existed between the top and the 50 foot level.

Considerable attention has been directed toward the prediction of peak surface wind gusts during thunderstorms. Fawbush and Miller (1954) developed an empirical technique for forecasting maximum surface wind speed. Their method, called the downrush temperature technique, was based on Brancato's (1942) discovery that temperatures of downdrafts reaching the surface in thunderstorms are approximately equal to the surface temperature of the moist adiabat through the intersection of the environmental wet-bulb curve and the zero degree isotherm.

Foster (1958) devised a method based on the buoyancy equation to compute the vertical velocity in a downdraft. This calculated downdraft velocity was then correlated with peak wind gusts at the surface. The correlation coefficient of 0.5 was disappointingly small, but it was statistically significant at the one percent level. To test the hypothesis that the downdraft transported upper-level momentum to the surface, the average wind speeds at 500 and 700 millibars were added to the computed downdraft velocity. This addition yielded an improvement in the correlation coefficient of only 0.01. Therefore, little useful information had been added.

Feteris (1965) extended Foster's and Fawbush and Miller's techniques by considering combinations of parameters rather than single parameters as predictors. An important parameter was the instability index, ΔT ,

defined as the difference between Fawbush and Miller's downrush temperature and the ambient air temperature at the surface. When ΔT was less than zero, a strong relation existed between maximum wind speed at the surface and mean vertical wind shear in the troposphere. This relationship supported the hypothesis that transfer of momentum from the middle and upper troposphere occurred under convectively unstable conditions. The results of the multiple linear regression analysis indicated that the combination of ΔT and the surface geostrophic wind speed explained the largest percentage of the variance. On the other hand, the predictors suggested by Fawbush and Miller explained very little variance of the peak wind gust.

Miller (1967) stated that the downrush temperature technique was not designed for tropical-type thunderstorms. Because the wet-bulb zero degree isotherm intersection in the subtropics during the summer is well above 10,500 feet, air from this level seldom reaches the surface. Consequently, this technique gives forecasts of wind speed which are too high. Miller also indicated that the dry instability index showed promise in predicting maximum gust speeds in regions where thunderstorm development is primarily associated with surface heating.

In 1965, data from a micrometeorological network of 14 towers equipped with wind sensors at various levels were used to test the downrush temperature technique at Cape Kennedy, Florida (Aerospace Review, 1965). Although this technique tended to overpredict peak wind gusts, it did prove to be useful as a forecast aid. The results from this study also pointed to the complexity of the problem of predicting peak winds

associated with individual thunderstorms. The regions of high winds were extremely localized and sharply edged. Thus a very dense observational network is necessary in order to accurately verify prediction methods.

Hiser, Senn and Courtright (1970) attempted to relate strong winds in tropical thunderstorms to radar parameters. Peak gusts were correlated with echo features including cell movement, age of storm, horizontal and vertical size, growth rates of the thunderstorm top and intensity of radar return. Although no single echo parameter could be used to identify all severe wind cases in south Florida, a combination of parameters showed promise.

Laboratory experiments have provided a useful analogy between atmospheric gust fronts and density currents. Simpson (1969) found similarities between the intrusion of a saline solution into fresh water and thunderstorm outflows. In most gust fronts examined, internal Froude numbers (ratios of inertial to buoyancy force), were similar to those found in tank experiments.

Colmer (1971) summarized the characteristics of gust fronts in different parts of the world, including several examples from Oklahoma. The total wind vector change associated with Oklahoma gust fronts was much greater than in the Bedford, England or Belgian Congo gust fronts, due to both the greater speed and greater direction changes. Analyses of the vertical cross sections of wind speeds of 13 gust fronts indicated that only five resembled Simpson's laboratory density current model which showed a lag near the lower boundary. Colmer suggested that this lag occurs only intermittently, being destroyed by cold dense air from aloft, then

reforming due to surface stress. The average gust size (wind speed increase) showed an increase with height in the lower layer (about 500 m), with most of this increase occurring in the first 50 m. The average gust length (the distance over which the gust size occurred) showed a slight decrease with height. Wind direction shifts were nearly constant with height in most of the 13 gust fronts.

Larger gusts were associated with faster moving storms. Differences in the gust fronts were also related to differences in the age of the storm. The gust front tends to occur close to the storm center while the storm is in the developing and mature stages, and then moves further ahead during the decaying stages. On the average, the wind shift line preceded the gust front by only a few minutes. The gust size varied in a direction parallel to the gust front, with the maximum occurring close to the projected storm track.

A three-dimensional analysis of a severe gust front associated with the Oklahoma squal line of May 31, 1969, was presented by Charba (1972). A windshift and pressure jump preceded the cold air outflow. Charba suggested that this pressure discontinuity was the result of a gravity wave jump. A projecting nose, similar to those found in laboratory currents, occurred about 750 m above the ground. It was also demonstrated that the gust front was dynamically similar to theoretical and experimental gravity currents by the near-equal values of the internal Froude numbers.

The results of previous investigations that have attempted to develop prediction schemes for the peak wind gust in a thunderstorm have been only partially successful in isolating those processes or parameters

that are important in the determination of the gust speed. Even the best results explained only sixty-six percent of the variance (Feteris, 1965). This disappointingly low value points to the complexity of the thunderstorm and the associated thunderstorm gust front. The circulations associated with thunderstorms are fully three-dimensional, non-linear, and non-steady. Energy sources and sinks are large. The primary causes of thunderstorms may differ from storm to storm. The environments may also be quite different. Therefore, it is not suprising that no single parameter explains very much of the variance in thunderstorm peak wind speeds.

1.3 Specific Goal of This Research

In order to predict accurately the maximum wind speed associated with any given thunderstorm, it would probably be necessary to develop a time-dependent, three-dimensional model capable of interacting with its environment. Such a model would require a representation of the important cloud physics as well as the cloud dynamics. Development of such a model would require an extremely large expenditure of money and effort, and is clearly outside the scope of this thesis. Instead, we investigate the time-dependent vertical structure of three Florida gust fronts and compare these subtropical storms with three continental severe storms in an effort to ascertain whether any simple, general properties of the wind structure exist. We further attempt to relate statistically any general properties of the wind structure to measurable synoptic and/or radar parameters utilizing data from Tampa, Florida.

2.0 THE OBSERVATIONS

2.1 Kennedy Tower Data

NASA's 150 m meteorological tower at Kennedy Space Center is located within Complex 39 Area on Merrit Island. There are no man-made structures or natural obstacles within several hundred feet of the tower which would cause unrepresentative disturbances in the ambient air flow. Wind speeds and directions were measured at 0.1 second intervals by means of dual-mounted sensors with the aid of a wind selector which automatically selected the proper side of the tower for recording. The data were collected at heights of 18, 30, 60, 90, 120 and 150 m and recorded on magnetic tape. Additional information concerning the 150 m tower is given in NASA Technical Memorandum X-53699.

The recorders were activated only when it seemed likely that a thunderstorm would pass over the tower. From the recordings, one-second averages of the data were computed and time-height cross sections were constructed. An example of a one-second average, time-height cross section is shown in Figure 1. Wind information was made available for 21 situations. Of these, only three cases had strong, well-defined maxima which could be positively identified with a thunderstorm cell on the radar film obtained from Daytona Beach. Due to both the lack of temperature data and the great distance (50 mi) between Cape Kennedy and the Daytona Beach radar, it is impossible to say definitely that any or all of the three Kennedy wind increases are associated with gust fronts.

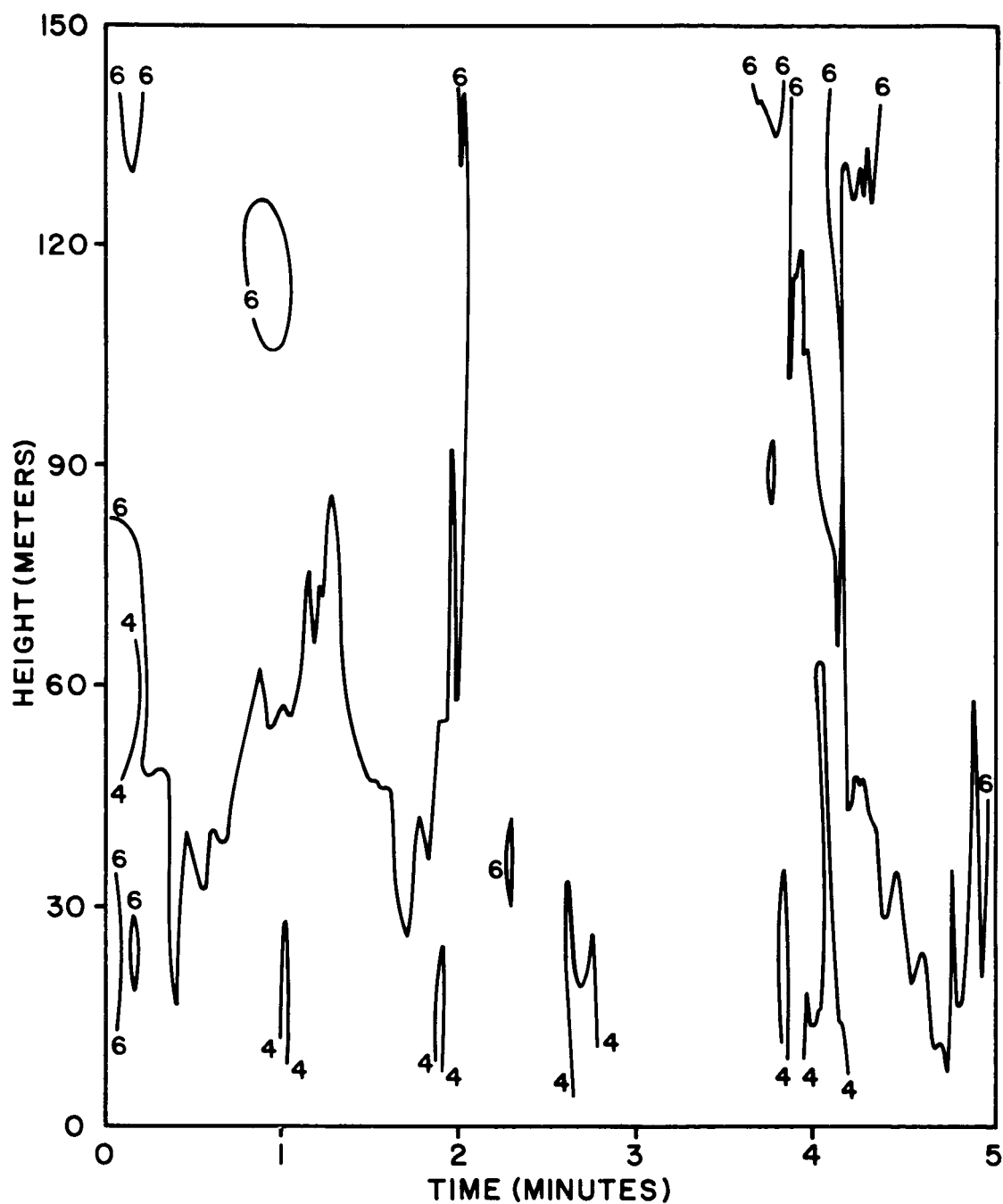


Figure 1. Time-height cross section of the one-second average wind speeds for the Florida gust front of July 27, 1967.

However, in this study, all wind speed increases such as those contained in these cases shall be referred to as the speed maxima associated with gust fronts.

2.2 NSSL-WKY Tower Data

To compare the gust fronts associated with Florida thunderstorms with more severe midwest thunderstorms, three severe thunderstorm gust front wind records were obtained from the National Severe Storms Laboratory at Norman, Oklahoma. Wind data for these three cases were recorded at the WKY television tower which is also used by the National Severe Storms Laboratory (NSSL) for meteorological data collection. This tower is located approximately seven miles north-northeast of downtown Oklahoma City and 23 miles north of Norman, Oklahoma. The surrounding area is relatively undeveloped. The wind sensors are Bendix-Friez aerovane wind transmitters mounted on booms at heights of 7, 44.5, 90.5, 177.1, 266.2, 355.4, and 444.6 m. The signals from the aerovanes are recorded by analog wind recorders operating at six inches per hour. A more detailed discussion of the WKY tower is contained in the NSSL Technical Memorandum #50.

2.3 Tampa Data

The three Florida cases and the three Oklahoma cases comprise the gust front sample from which the vertical and temporal variation of the wind speeds during the passage of a typical gust front is inferred. It will be shown that wind information near the surface is sufficient to infer

winds at higher levels.

The second part of this report is concerned with relating parameters near the surface which describe the gust fronts, such as the maximum wind speed, to synoptic scale and/or radar parameters. No tower is required for this analysis. Data were obtained from the National Climatic Center and were used in statistical analysis to determine the predictability of these descriptive parameters. These data consisted of surface weather observations, radar observations, surface wind recorder charts (1200Z and 0000Z of the following date), winds aloft and rawinsonde temperature and humidity information (1200Z and 0000Z of the following date) for 81 storms at Tampa, Florida. The data spanned the summers (June through September) of 1967 through 1971.

3.0 ANALYSIS OF TOWER DATA

3.1 Relevant Time Scales

Before describing the analysis of the tower data, it is important to define the relevant time scales associated with the gust front. In general, atmospheric circulation features are categorized by three main time scales, the synoptic scale of a few days, the mesoscale of a few hours, and the microscale of a few seconds to minutes. From inspection of many times series of wind speeds during the passage of a thunderstorm gust front, there appear to be at least two distinct time scales. One is associated with the microscale turbulence and has a characteristic period of a few seconds. The other is associated with the organized longer-lived circulation of the thunderstorm itself and has a typical period of about 20-30 minutes. This period is obviously related to the time scale associated with individual convective elements.

The latter time scale is of primary interest in this study. For example, Figures 2a, 3a, and 4a show 130-second average time-height cross sections of wind speed at Cape Kennedy during the passage of three thunderstorm gust fronts. The prominent feature in each figure is the wind speed jump from a minimum to a maximum. Associated with this increase, ΔV , is a time interval, Δt . The average Δt for the wind increase in all six gust front cases was about 11 minutes. The values of Δt and ΔV are believed to be the most important characteristics needed for gust prediction. The higher frequency oscillations will be considered essentially random and unpredictable.

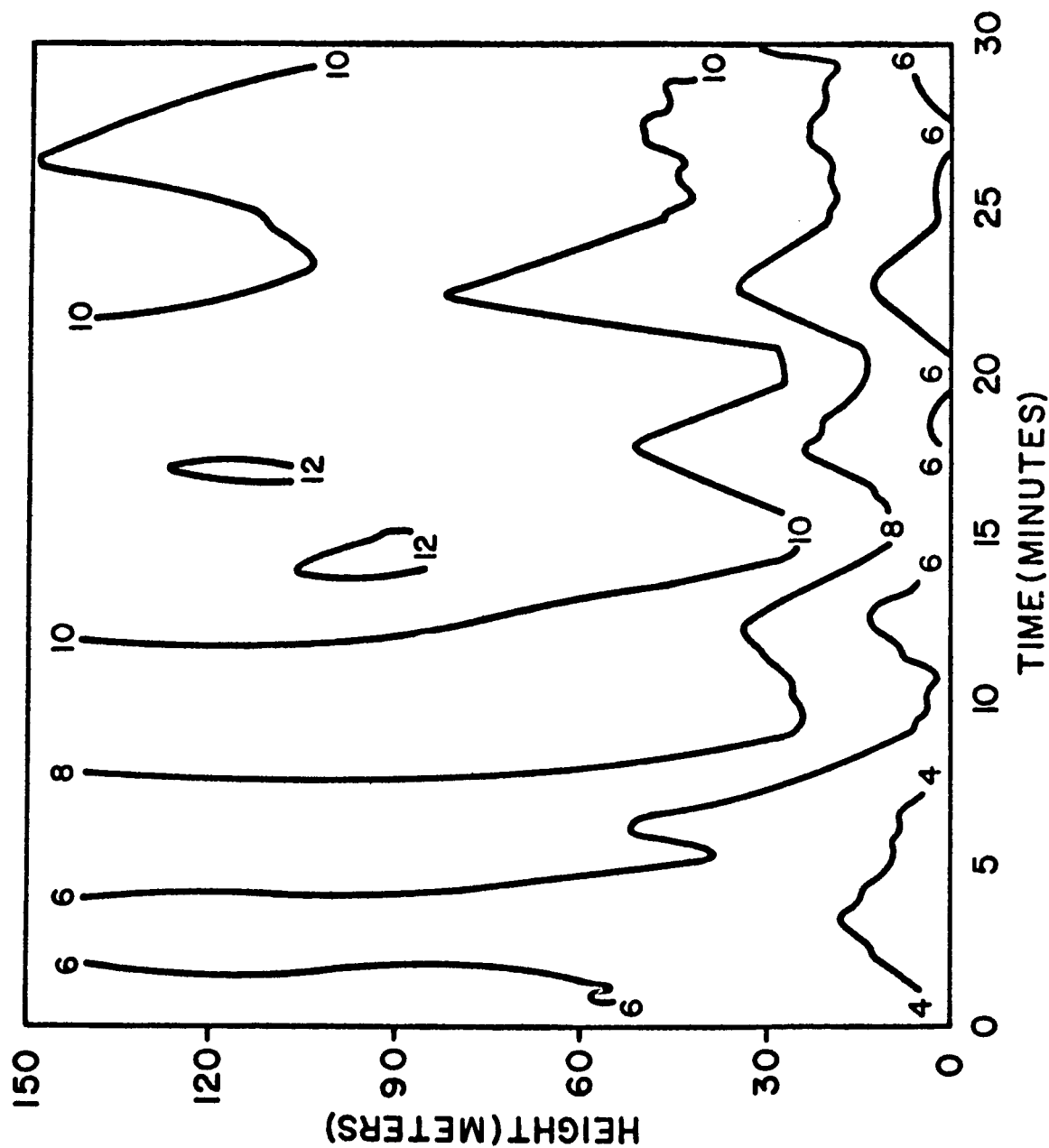


Figure 2a. Time-height cross section of the 130-second running mean of wind speeds for the Florida gust front of July 27, 1967. The isotachs in this figure are expressed in mps.

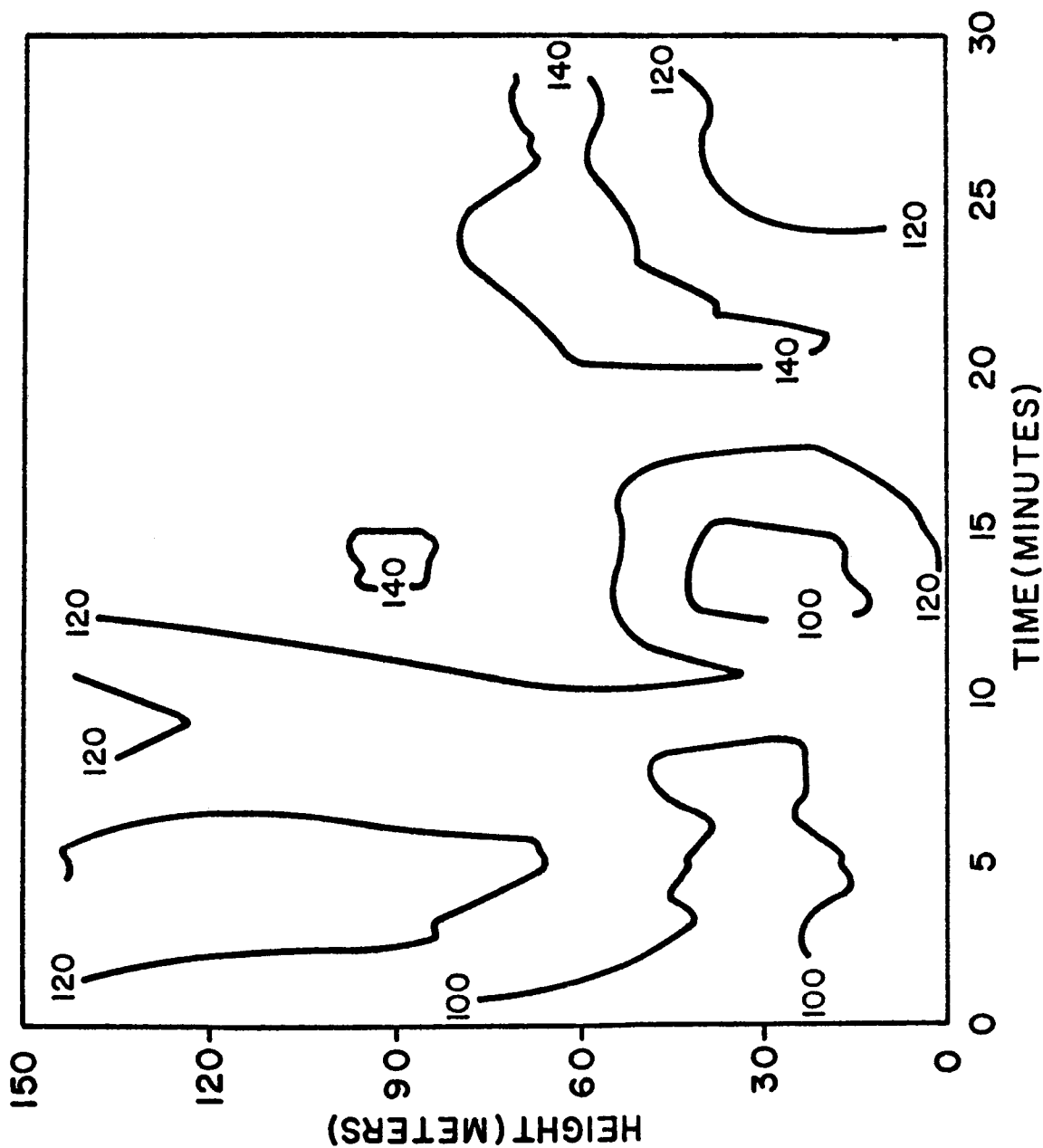


Figure 2b. Time-height cross section of the 130-second running mean of wind directions for the Florida gust front of July 27, 1967. The isogons in this figure are expressed in degrees.

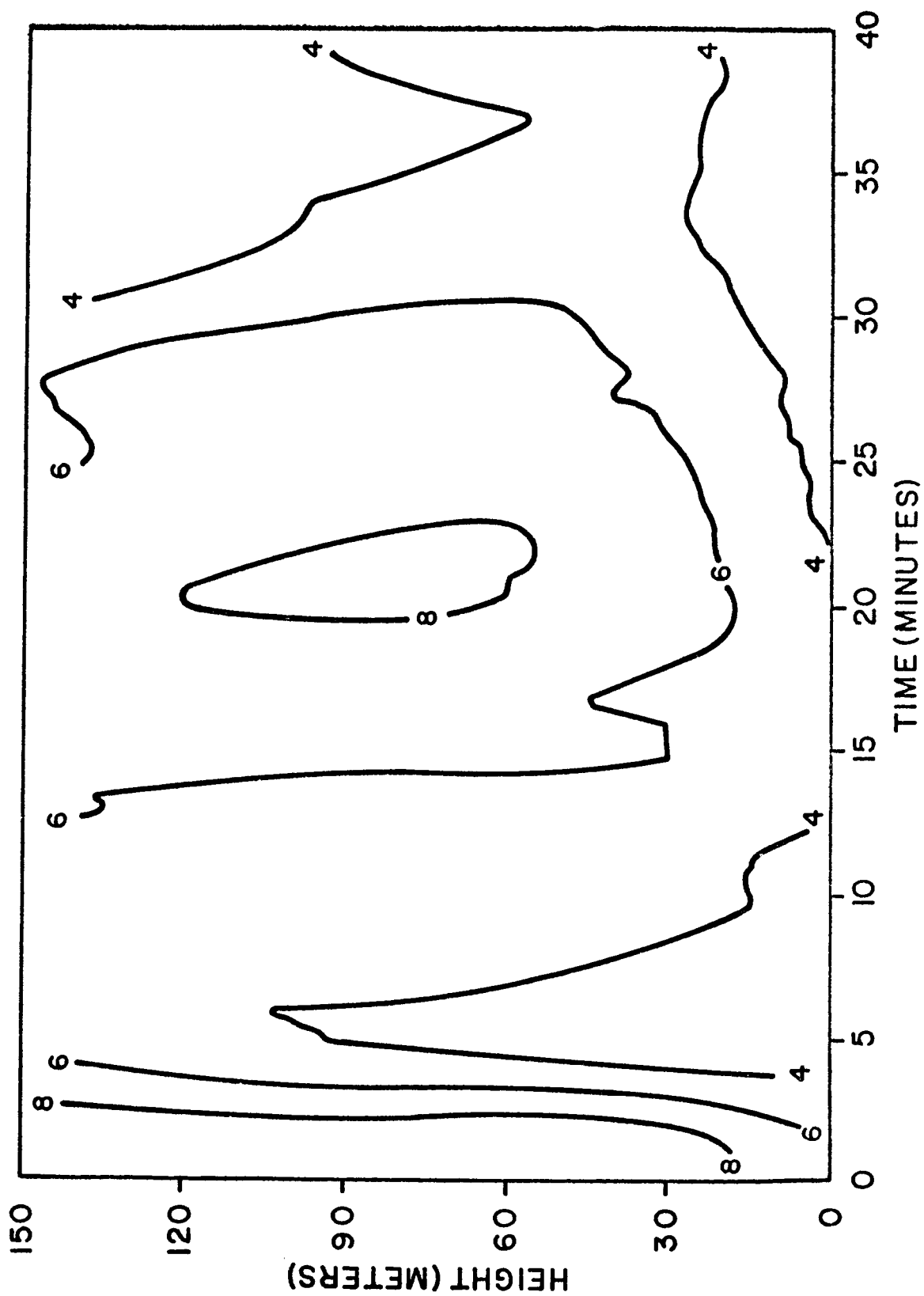


Figure 3a. Time-height cross section of the 130-second running mean of wind speeds for the Florida gust front of April 29, 1968. The isotachs in this figure are expressed in mps.

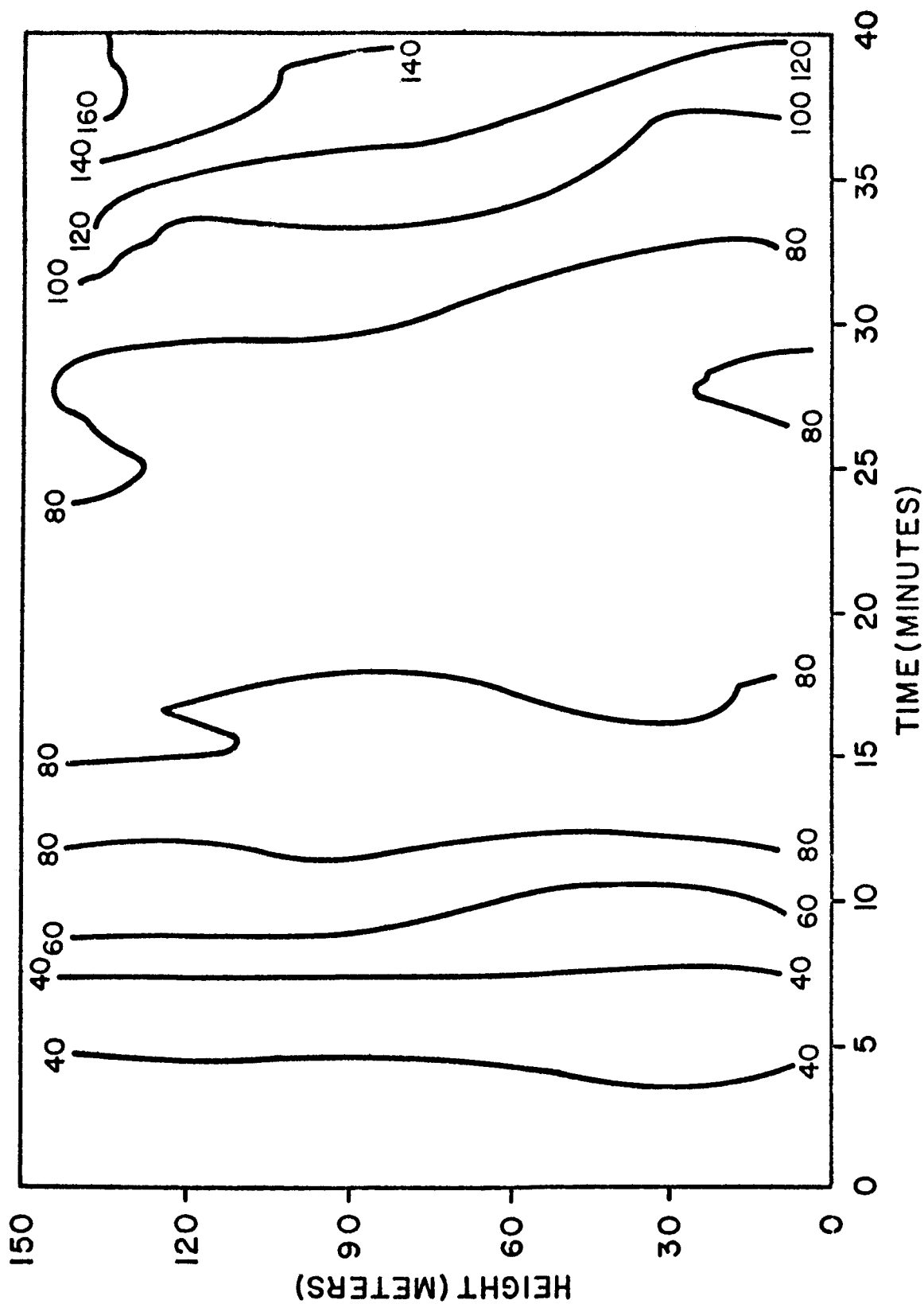


Figure 3b. Time-height cross section of the 130-second running mean of wind directions for the Florida gust front of April 29, 1968. The isogons in this figure are expressed in degrees.

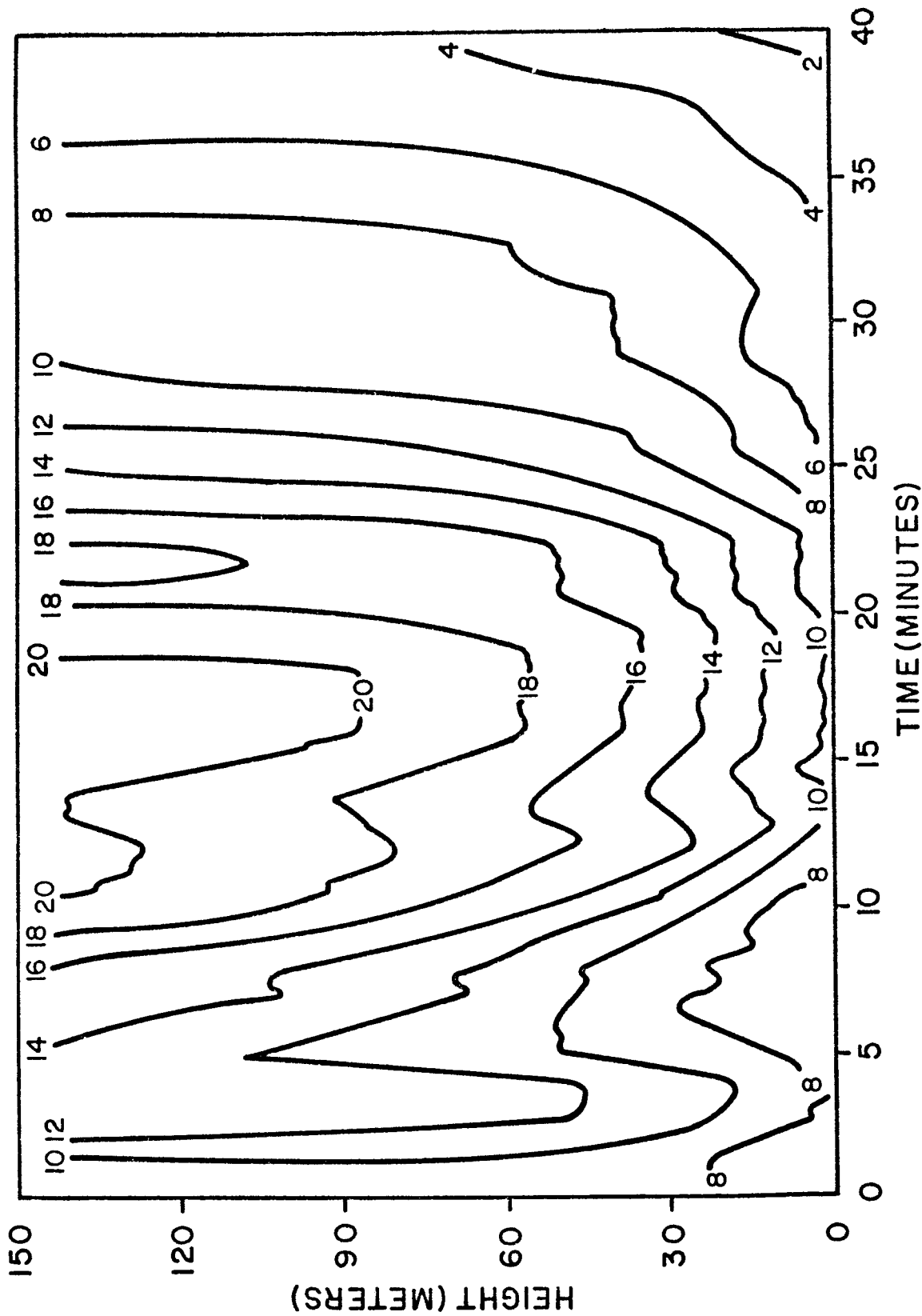


Figure 4a. Time-height cross section of the 130-second running mean of wind speeds for the Florida gust front of June 25, 1968. The isotachs in this figure are expressed in mps.

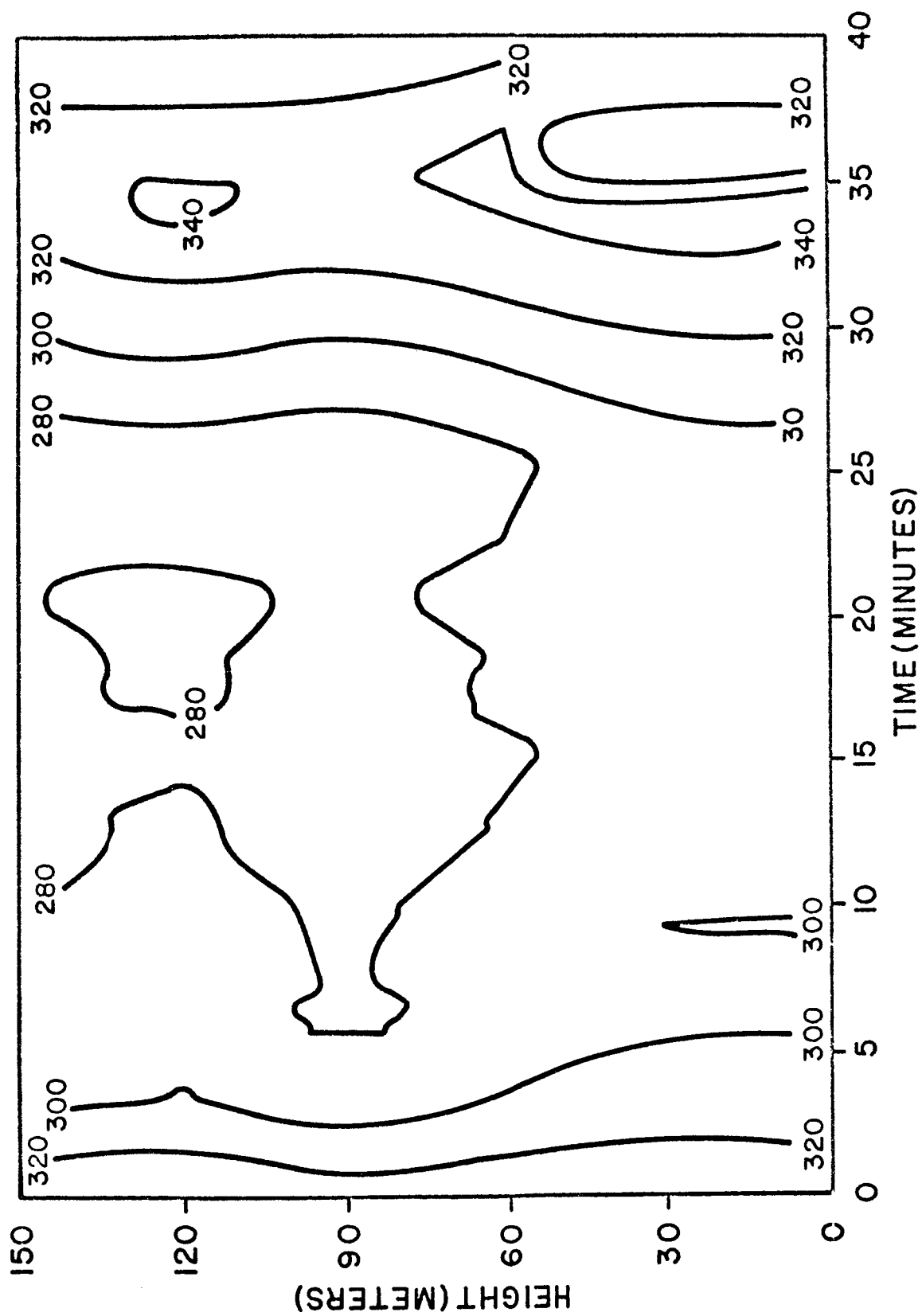


Figure 4b. Time-height cross section of the 130-second running mean of wind directions for the Florida gust front of June 25, 1968. The isogons in this figure are expressed in degrees.

3.2 Smoothing the Wind Data

The original wind data for the Florida cases consisted of data at 0.1-second intervals stored on magnetic tape, which had been averaged over one-second periods. To isolate the variations in wind associated with the longer time scale, 130-second moving averages were computed every ten seconds.

The original Oklahoma data consisted of strip charts of wind traces recorded at the rate of six inches per hour. These traces were first smoothed manually. Time-height cross sections were then constructed by selecting wind speeds at 2.5-minute intervals. These analyses are presented in Figures 5, 6, and 7.

Although a sampling interval of 2.5 minutes is rather long to represent a phenomenon with a period of about 20 minutes, prior smoothing of the time series should reduce the effect of aliasing on the analyses.

The smoothed time-height cross sections (Figures 2-7) formed the basis for subsequent analysis. A brief qualitative description of the six gust fronts follows in the next section.

3.3 Summary of the Six Gust Front Cases

Following Colmer (1971), the parameters ΔV (magnitude of wind increase) and Δt (length of time interval over which the wind increases) are defined as the gust size and gust length respectively. If the speed of the advancing gust front, C , is constant, the spatial distance from the wind minimum to the wind maximum may be found by multiplying Δt by C . Several of the important parameters which characterize the six gust front

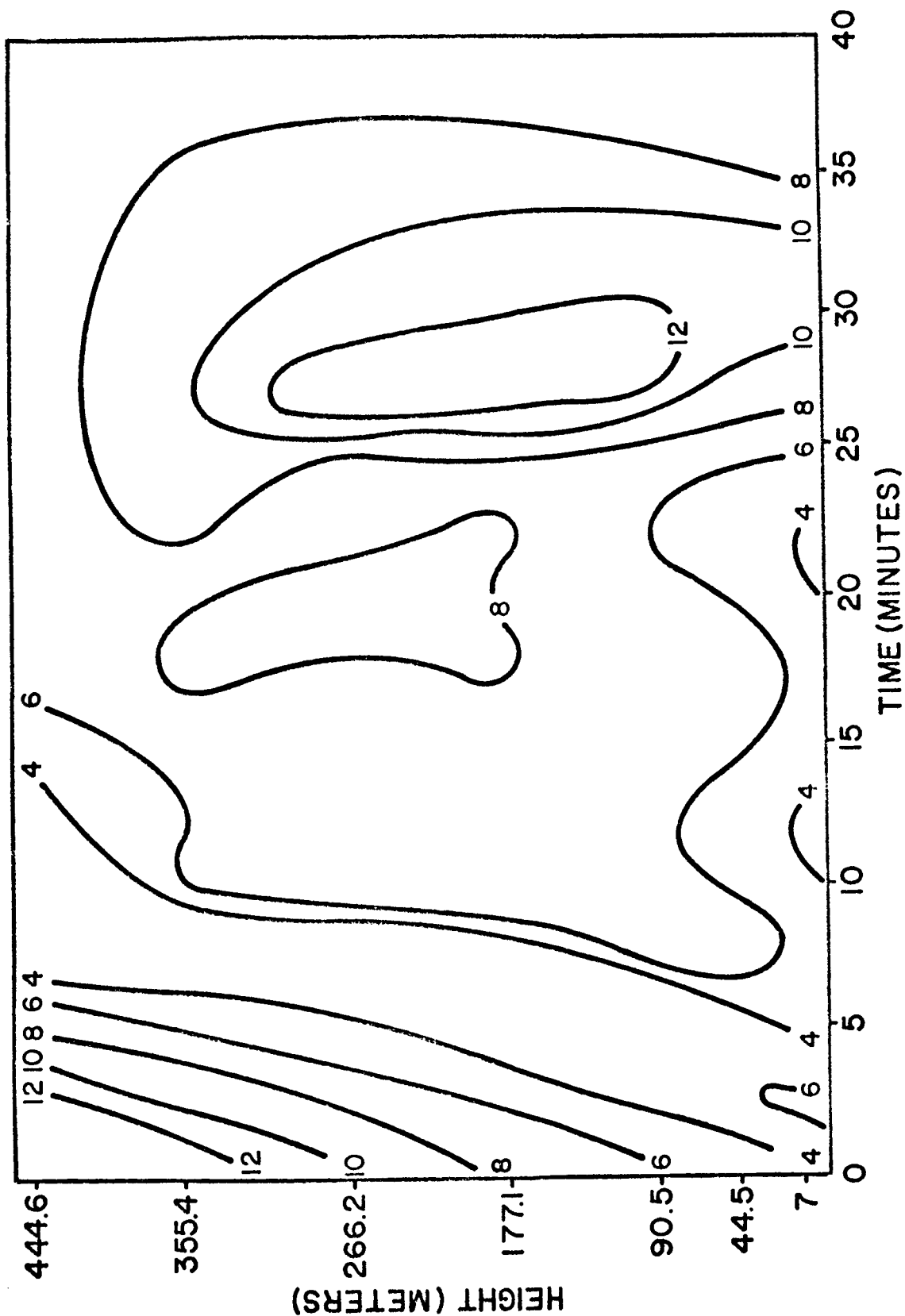


Figure 5. Time-height cross section of the hand-smoothed wind speeds for the Oklahoma gust front of April 16, 1969. The isotachs in this figure are expressed in mps.

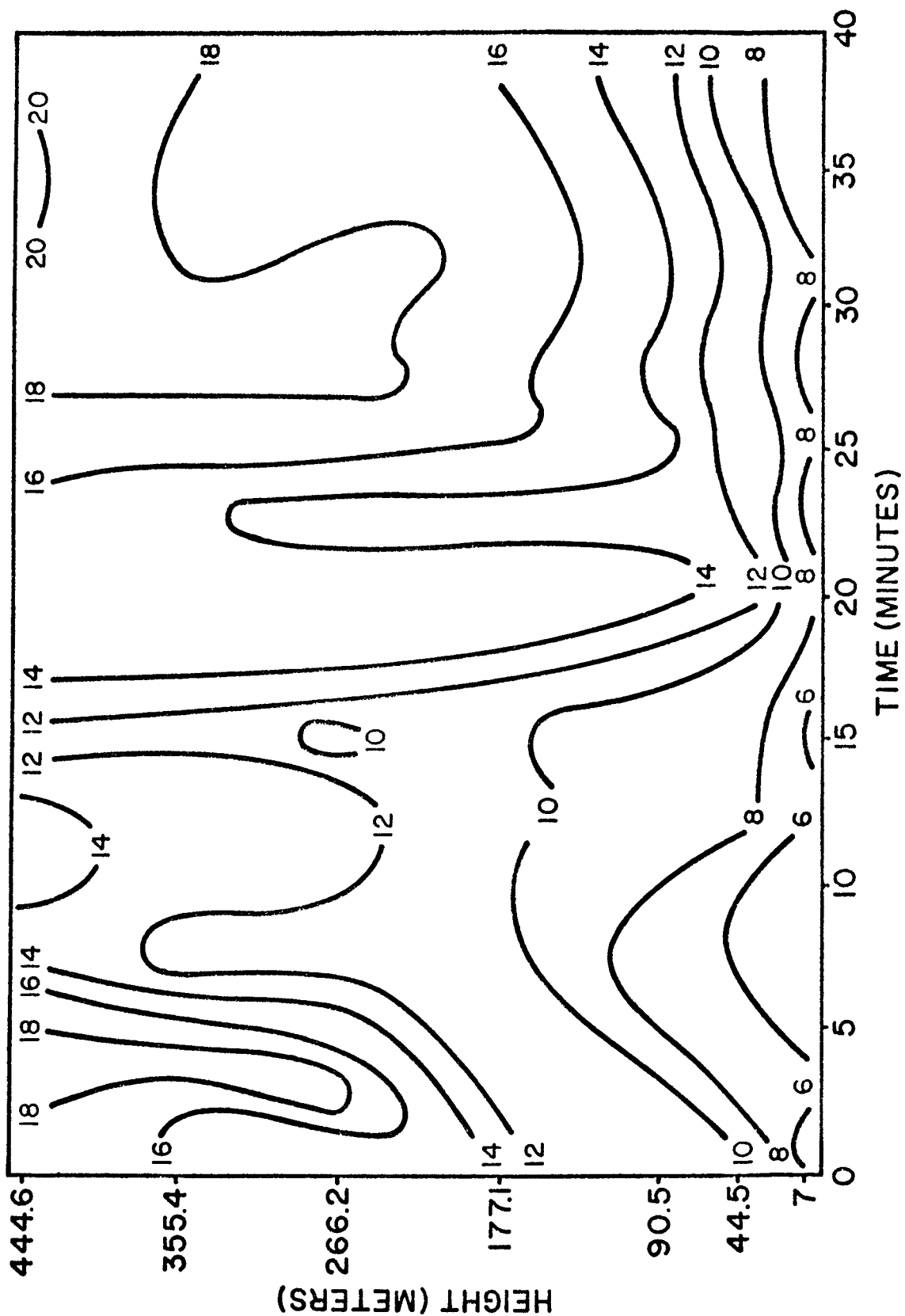


Figure 6. Time-height cross section of the hand-smoothed wind speeds for the Oklahoma gust front of April 26, 1969. The isotachs in this figure are expressed in mps.

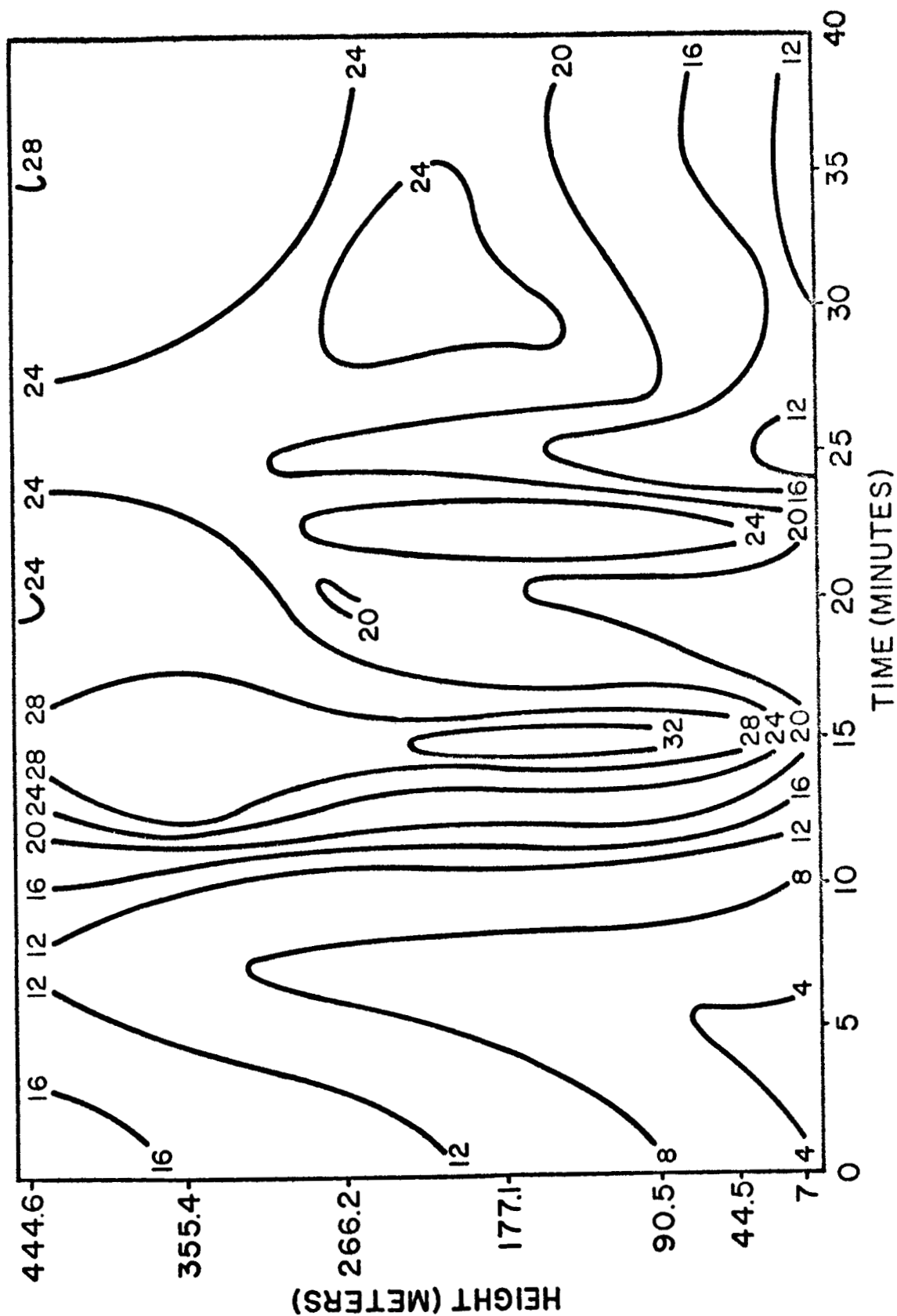


Figure 7. Time-height cross section of the hand-smoothed wind speeds for the Oklahoma gust front of May 31, 1969. The isotachs in this figure are expressed in mps.

cases are presented in Table 1. These parameters include: 1) maximum wind speed; 2) gust size at 18 m; 3) gust size at the height of the maximum wind; 4) gust length at 18 m; 5) gust length at the height of the maximum wind; 6) the slope of the peak gust axis.

In spite of the differences among the six gust front cases, several similarities may be noted. In five out of six cases, the gust size increased with height and the gust length decreased with height. These results agree with the average properties found by Colmer (1971).

In all six cases, the axis of the maximum wind was nearly vertical. Both slight upstream and downstream slopes existed, but no preferred direction was evident. In all cases, the vertical wind shear increased over the gust length and reached a maximum at the time of maximum wind.

The variation from case to case in slope of the peak gust axis as well as the gust front itself and the variation in gust length with height are probably results of surface friction. Colmer suggested that a lag in the gust front near the ground occurs intermittently, so that the denser cold air aloft spreads out ahead of the surface portion of the gust front. Turbulent mixing tends to destroy the overhanging bulge as the dense air sinks toward the surface. The lag then reforms through the effect of surface drag. These two non-steady processes in the immediate vicinity of the gust front may lead to small slopes in either the upstream or downstream direction at any time, and they are unpredictable for a particular storm at a particular location.

Table 1. Values of descriptive parameters for the six gust fronts.

	GUST FRONT	PEAK WIND IN THE GUST (mps)	GUST SIZE AT 18 m (mps)	GUST SIZE AT HGT OF THE PEAK WIND (mps)	GUST LENGTH AT 18 m (seconds)	GUST LENGTH AT HGT OF PEAK WIND (seconds)	APPROX. SLOPE (m/min)
FLORIDA	July 27, 1967	12+	5.3	7.3	12.0	11.5	164.8
	April 29, 1968	8+	3.4	5.1	13.5	15.5	-60.0
	June 25, 1968	20+	5.6	7.3	13.0	17.5	54.9
OKLAHOMA	April 16, 1969	12+	6.2	6.2	9.3	8.3	117.5
	April 26, 1969	14+	5.6	7.2	12.5	5.0	375.0
	May 31, 1969	32+	21.9	27.1	11.3	7.5	1125.0

4.0 MODELING THE THUNDERSTORM GUST FRONT

4.1 Scaled Time-Height Cross Sections

Differences in magnitudes of the gust size, gust length, and height at which the peak gust occurs make it difficult to draw general conclusions about the vertical structure of the wind speed associated with the six gust fronts. Scaled time-height cross sections were constructed in order to test the hypothesis that the gust fronts differ only in magnitude, but not in basic structure. Empirical scaling parameters for time, height, and velocity were used to construct non-dimensional time-height cross sections of velocity. For the time scaling parameter, an obvious choice is gust length Δt . The height scaling parameter was chosen to be the height at which the maximum wind occurred, ΔZ . The velocity scaling parameter was chosen to be the gust size, ΔV . Of the three scaling parameters, ΔZ was the most difficult to define. As indicated in the unscaled cross sections (Figures 2a, 3a, 4a, 5, 6, and 7), the maximum wind is elongated in the vertical, so that a precise definition of ΔZ is difficult. Also, in one Cape Kennedy case, the height of the maximum occurs above the top level of the tower; the height in this case could be estimated only approximately.

Figures 8, 9, and 10 show the scaled cross sections for the three Cape Kennedy cases. In contrast to the unscaled cross sections, the scaled gust front profiles are quite similar. The maxima of scaled velocities are all about 1.7 and occur at $Z/\Delta Z$ and $t/\Delta t$ of 1.0. These

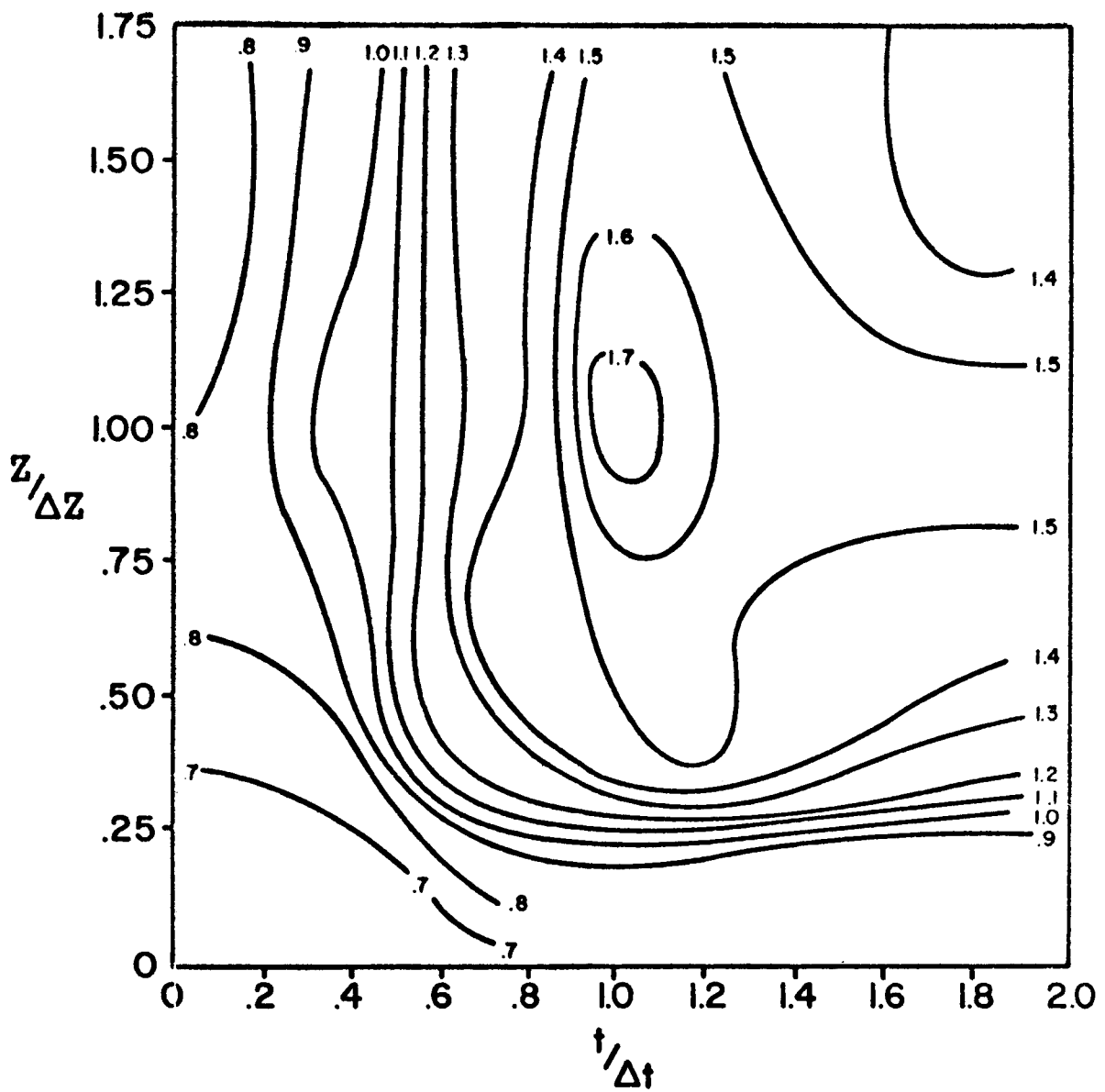


Figure 8. Scaled time-height cross section of wind speed for the Florida gust front of July 27, 1967.

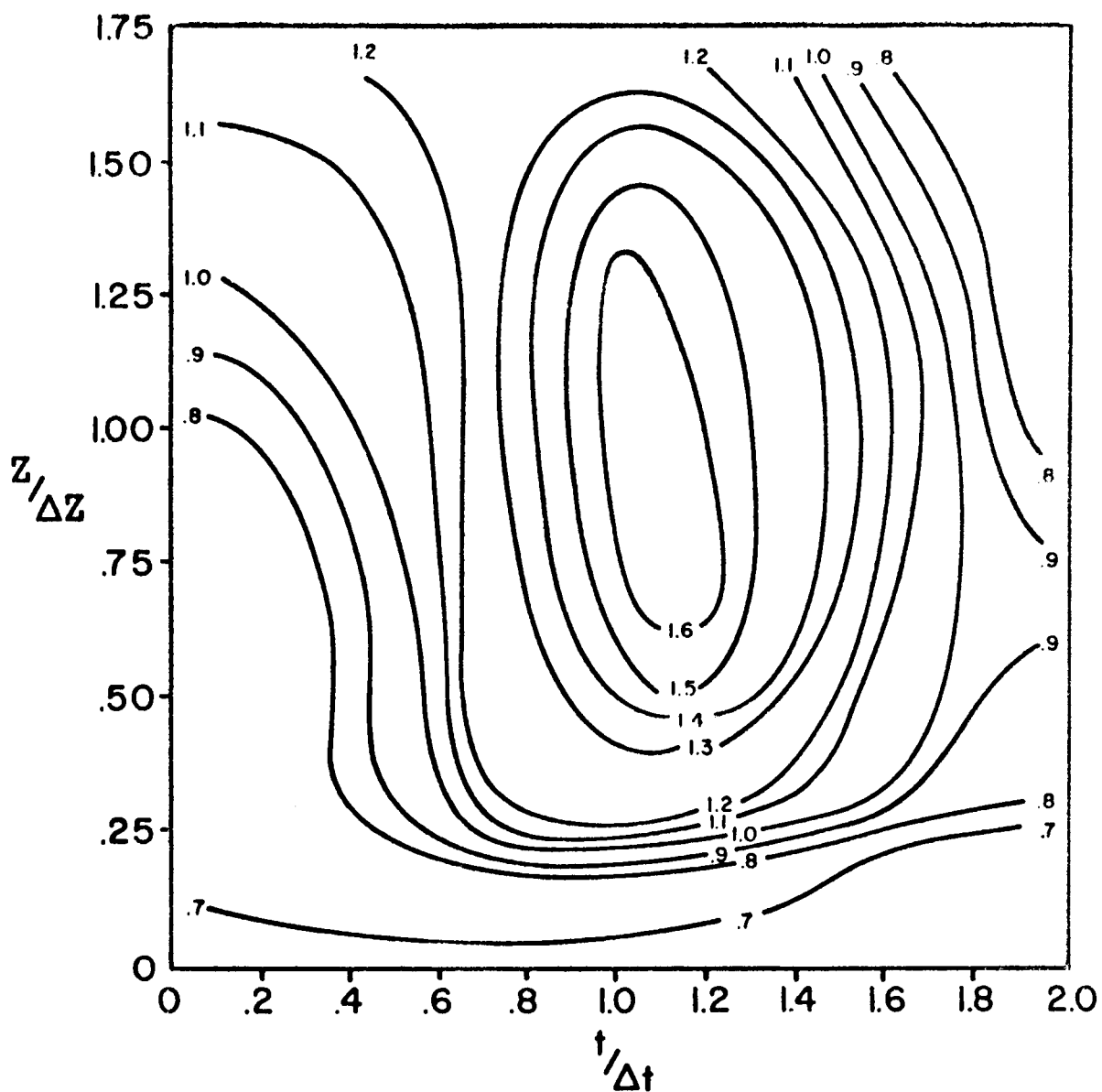


Figure 9. Scaled time-height cross section of wind speed for the Florida gust front of April 29, 1968

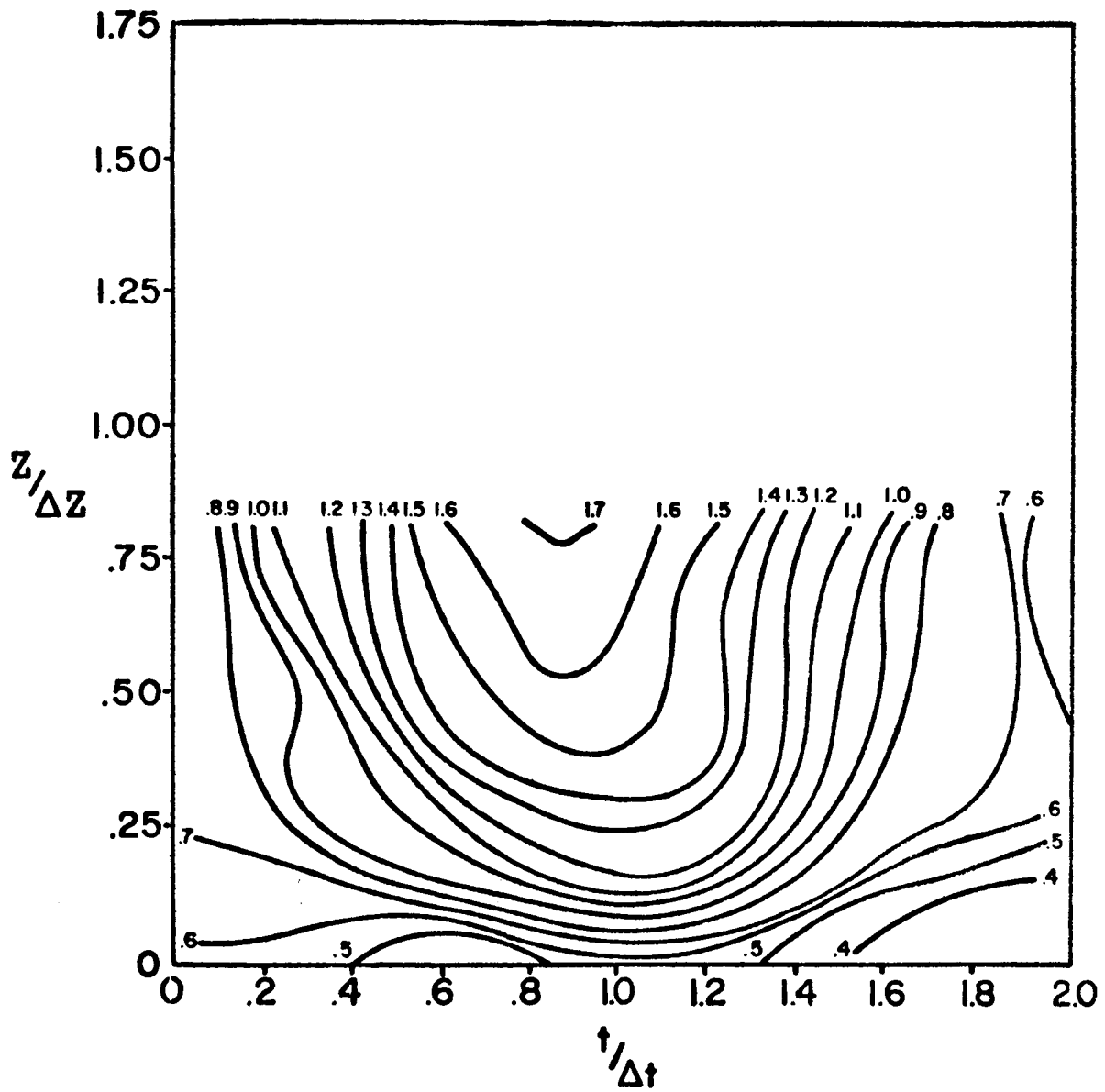


Figure 10. Scaled time-height cross section of wind speed for the Florida gust front of June 25, 1968.

results indicate that if the scaling parameters ΔV , Δt , and ΔZ are known, at least part of the wind structure of the gust front could be determined. The difficulty lies in predicting the scaling parameters, especially ΔZ . Considerable effort has been directed toward the prediction of peak surface wind gusts (which should be closely related to ΔV). The parameter Δt might be related to parameters such as cell size and speed of movement, which could be determined from radar. However, there is no obvious basis on which to choose ΔZ . For this reason, the effort to find a height scaling parameter was abandoned and a simple hypothesis to explain the wind structure was tested. This hypothesis was simply that the vertical variation of the wind at the time of maximum wind speed might follow the logarithmic wind law in the lower portion of the gust front, because logarithmic profiles are known to occur with strong winds (Blackadar et al., 1972).

4.2 Test of the Logarithmic Wind Law Hypothesis

The logarithmic wind law is derived with the assumption that Richardson number, is small, where

$$Ri = \frac{\frac{g}{\theta} \frac{\partial \theta}{\partial z}}{\left(\frac{\partial u}{\partial z}\right)^2 + \left(\frac{\partial v}{\partial z}\right)^2} \quad (4.1)$$

Here u and v are horizontal velocity components in arbitrary Cartesian directions. The Richardson numbers associated with the peak gust are undoubtedly small, regardless of the static stability, because of the

great wind shear. The logarithmic wind law states that the ratio of wind speeds (V_1 and V_2) at two different heights (z_1 and z_2) is a function only of the roughness length, z_0 .

$$\frac{V_2}{V_1} = \frac{\ln(z_2/z_0)}{\ln(z_1/z_0)} \quad (4.2)$$

The roughness length depends upon the upwind terrain. Therefore, at any one location, z_0 is a function of wind direction. Recent results (Blackadar et al., 1972) indicate that there is no systematic departure from the logarithmic wind law up to a height of about 150 m, which is higher than previously thought.

The first step in testing the validity of the logarithmic wind law was the construction of time-height cross sections of the ratio (V/V_{18}) of the wind speed to the speed at 18 m. If the logarithmic wind law is valid, then this ratio should be a function only of the roughness length, which may depend on wind direction, and also is different at Cape Kennedy and Oklahoma. In the construction of these cross sections, the time axis was scaled by Δt with the origin chosen as the time of the wind minimum prior to the gust front. Thus, the peak gust always occurs at $t/\Delta t = 1$. The 18 m wind speeds for Oklahoma were obtained by linear interpolation between the 7 m and 44.5 m levels. The resulting isopleth analyses are shown in figures 11-16.

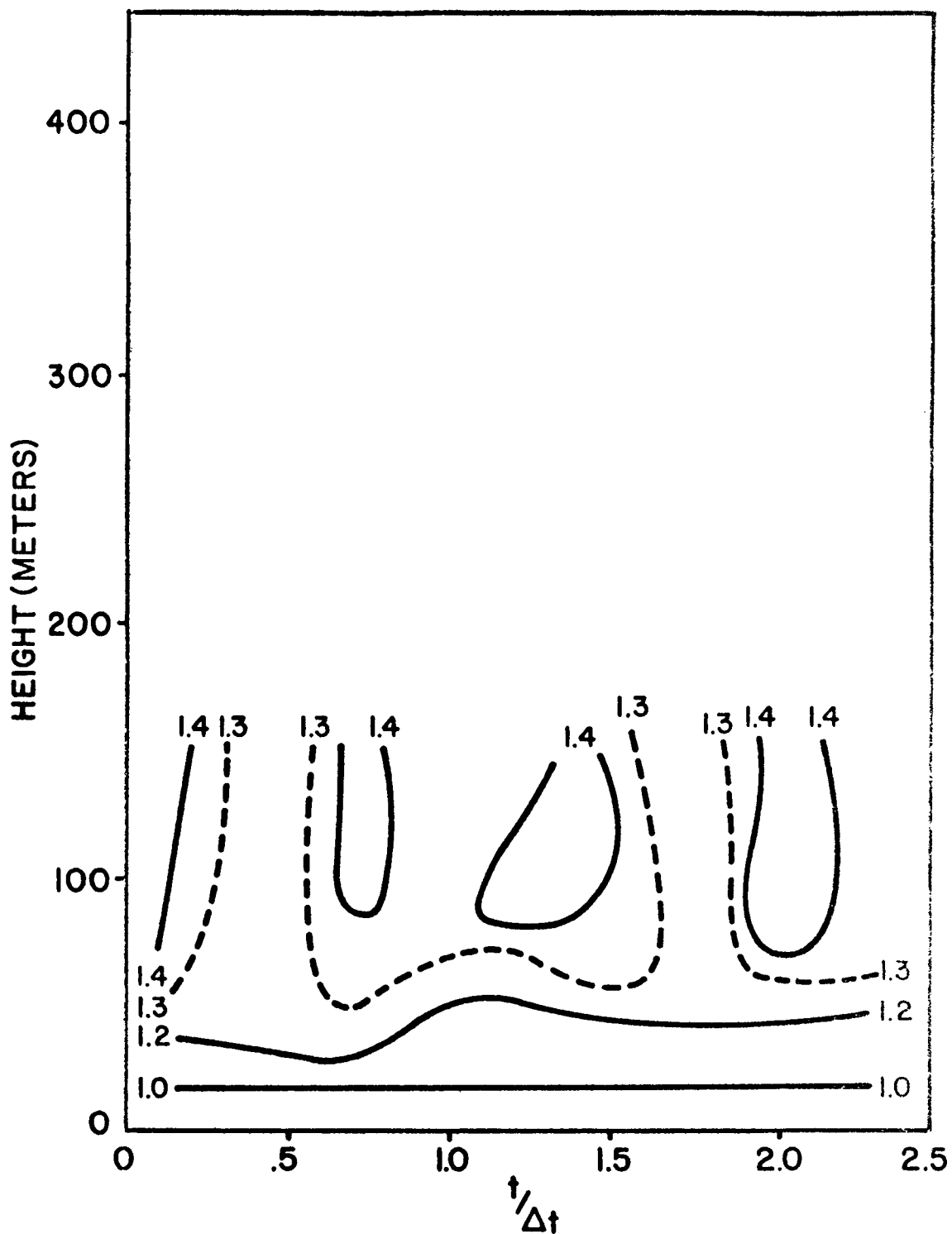


Figure 11. Ratio of wind speed to speed at 18 m vs. height and scaled time for the Florida gust front of July 27, 1967.

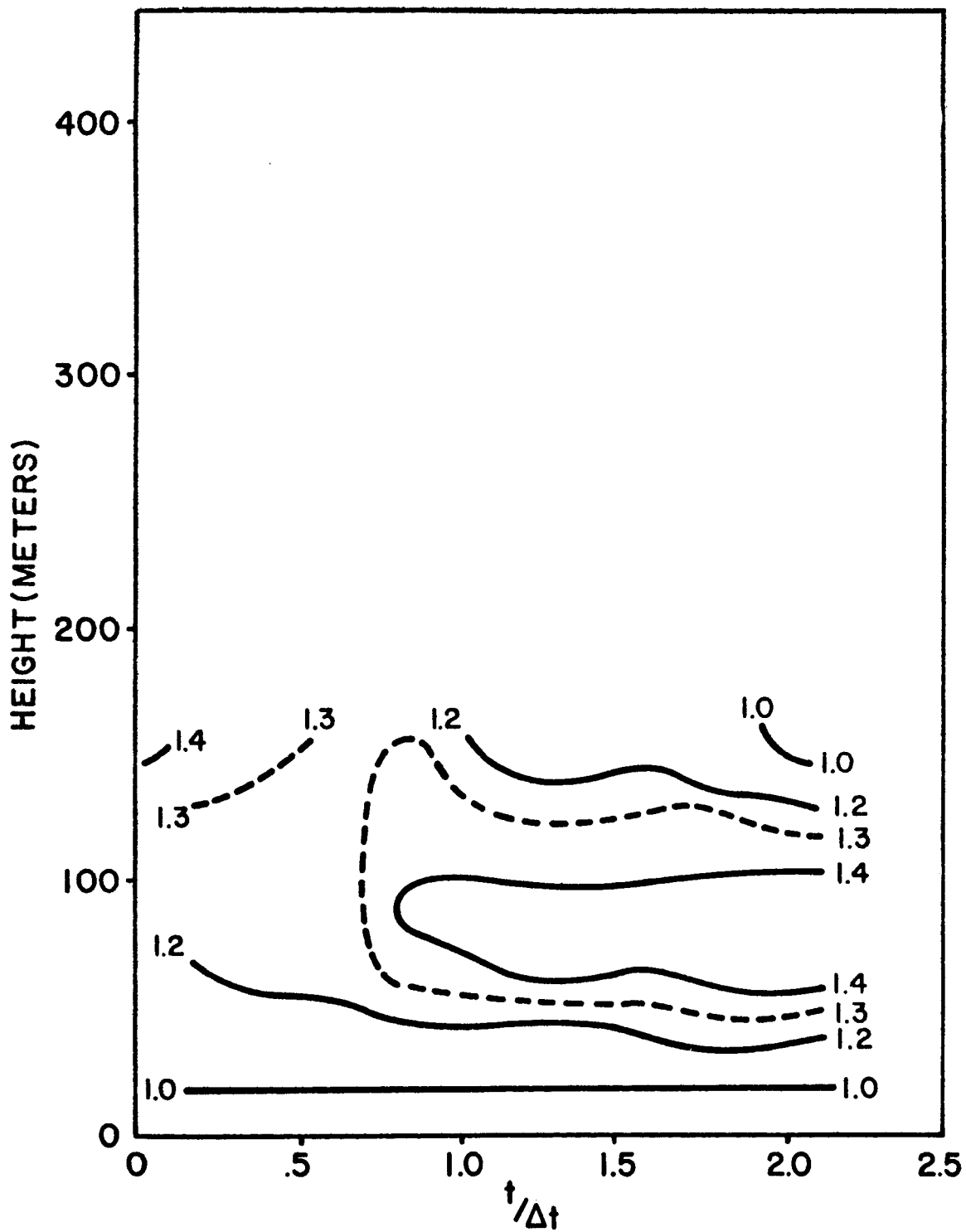


Figure 12. Ratio of wind speed to speed at 18 m vs. height and scaled time for the Florida gust front of April 29, 1968.

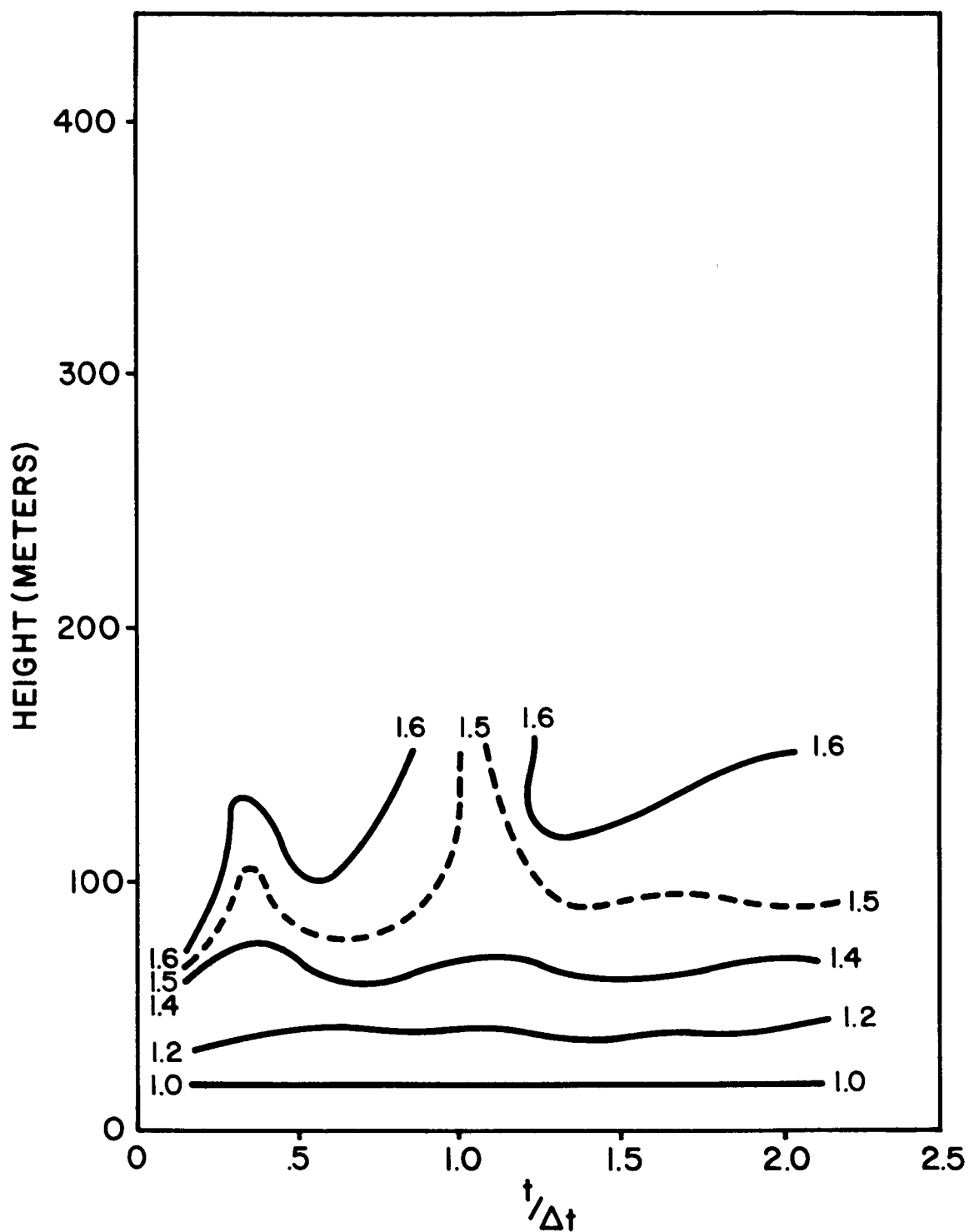


Figure 13. Ratio of wind speed to speed at 18 m vs. height and scaled time for the Florida gust front of June 25, 1968.

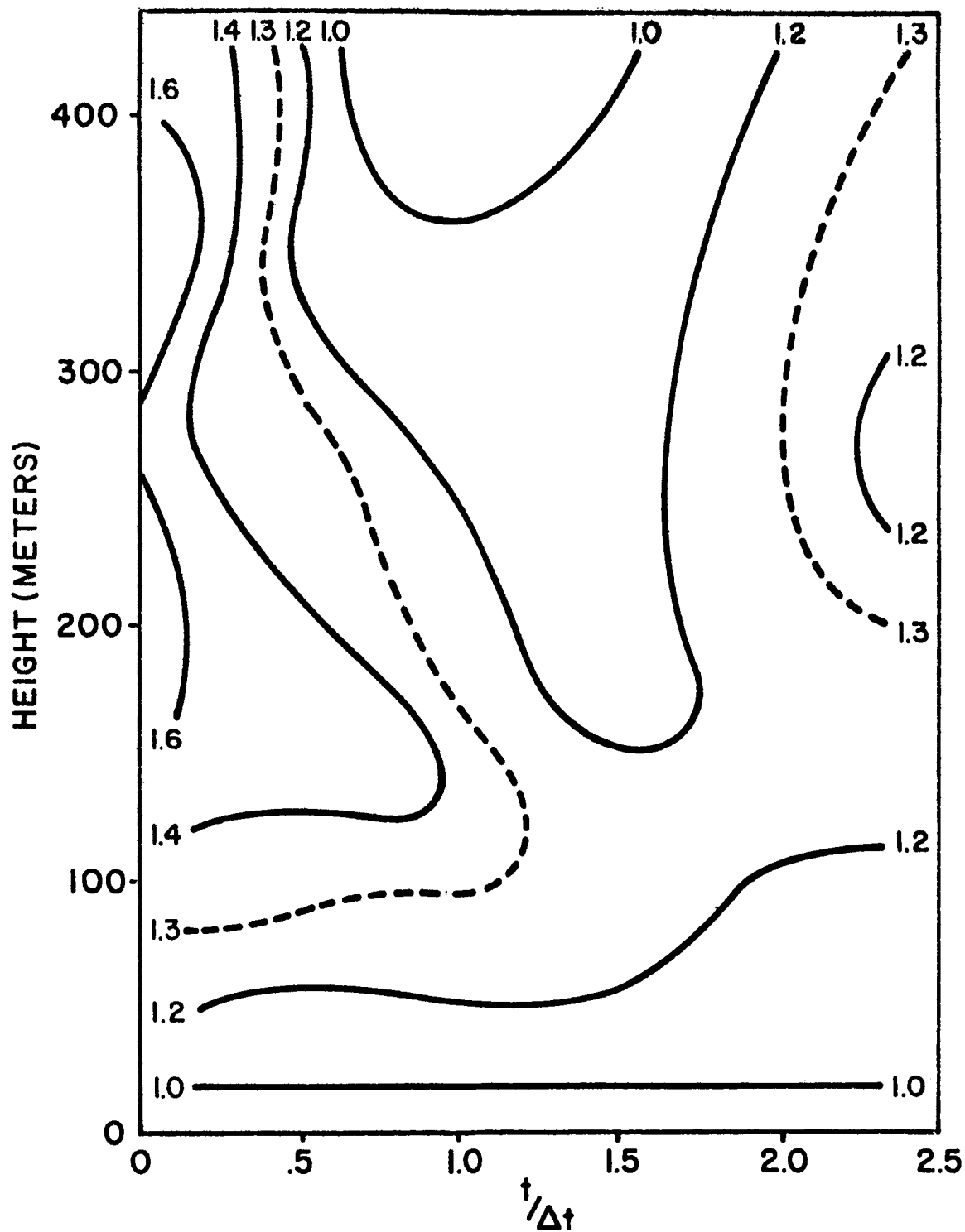


Figure 14. Ratio of wind speed to speed at 18 m vs. height and scaled time for the Oklahoma gust front of April 16, 1969.

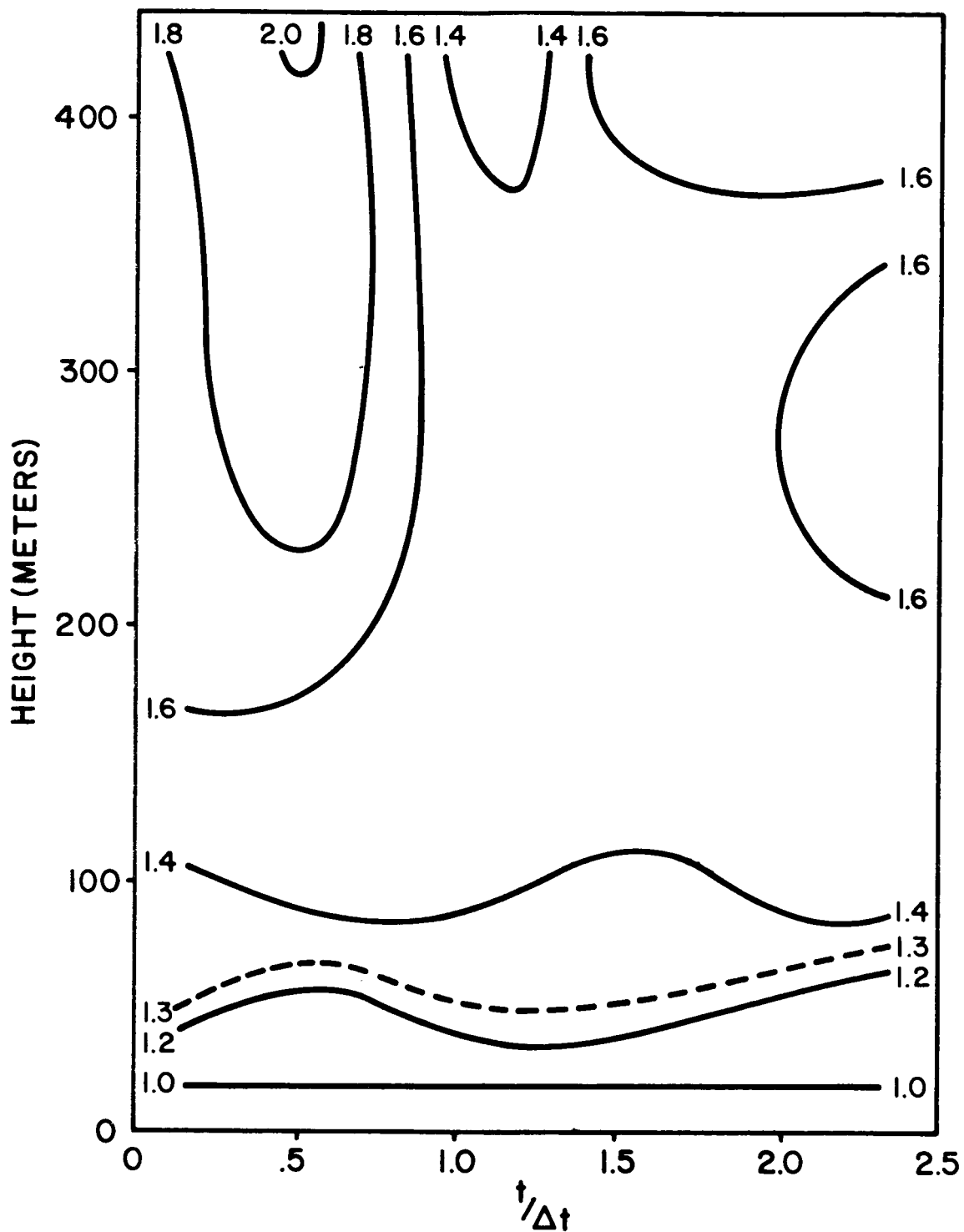


Figure 15. Ratio of wind speed to speed at 18 m vs. height and scaled time for the Oklahoma gust front of April 26, 1969.

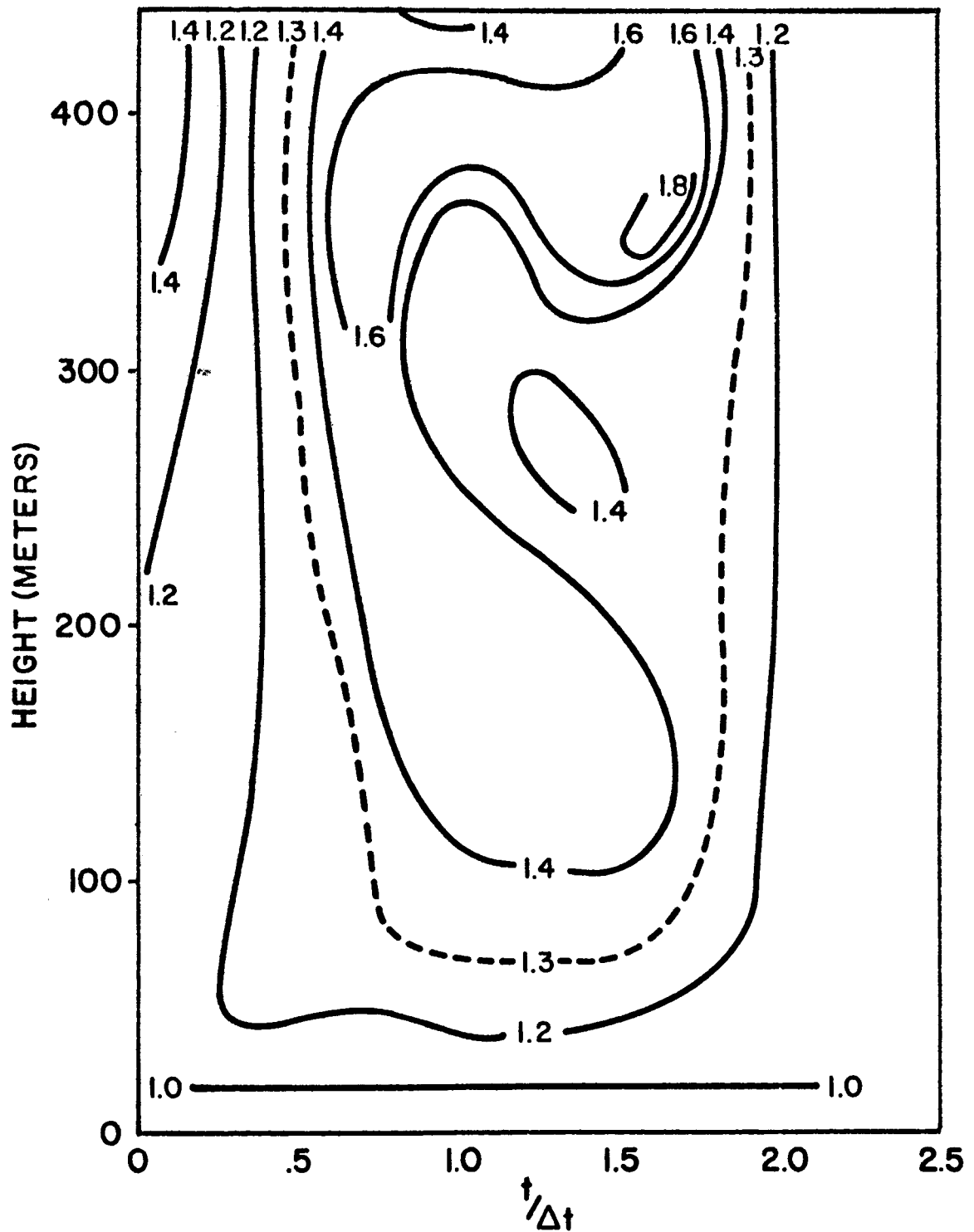


Figure 16. Ratio of wind speed to speed at 18 m vs. height and scaled time for the Oklahoma gust front of May 31, 1969.

The scaled velocities associated with the six scaled cross sections show several important similarities. The vertical shear is concentrated below 100 m, and the shear is relatively independent of time. Above 100 m, the structure is more complicated. On the average, the vertical shear is less. The several maxima and minima of shear above 100 m in most of the sections are not associated with the maxima and minima in actual wind speeds.

The scaled speeds in the three Oklahoma cases (Figures 14-16) show a greater range in the shear than the Florida cases. However, the range in the lower 150 m is about the same. Throughout the entire time interval, the shear in the lower levels is remarkably constant.

The nearly steady-state ratio of V/V_{18} in the lower 100 m of each gust front supports the tentative hypothesis that the logarithmic wind law is valid in this region. The next step in testing this hypothesis was to determine whether the differences in the ratios among the six cases could be explained on the basis of different roughness lengths.

4.3 Comparison of Roughness Lengths Under Thunderstorm Conditions

With Those Under Non-thunderstorm Conditions

In previous studies, Blackadar et al. (1972) and Sanders and Weber (1970) have empirically determined roughness lengths for the terrain around the Cape Kennedy and WKY Towers. Both studies were made under strong wind, but non-thunderstorm, conditions. Plots of the average z_0 , as a function of azimuth, from these studies are shown in Figures 17 and 18 for Cape Kennedy and Oklahoma.

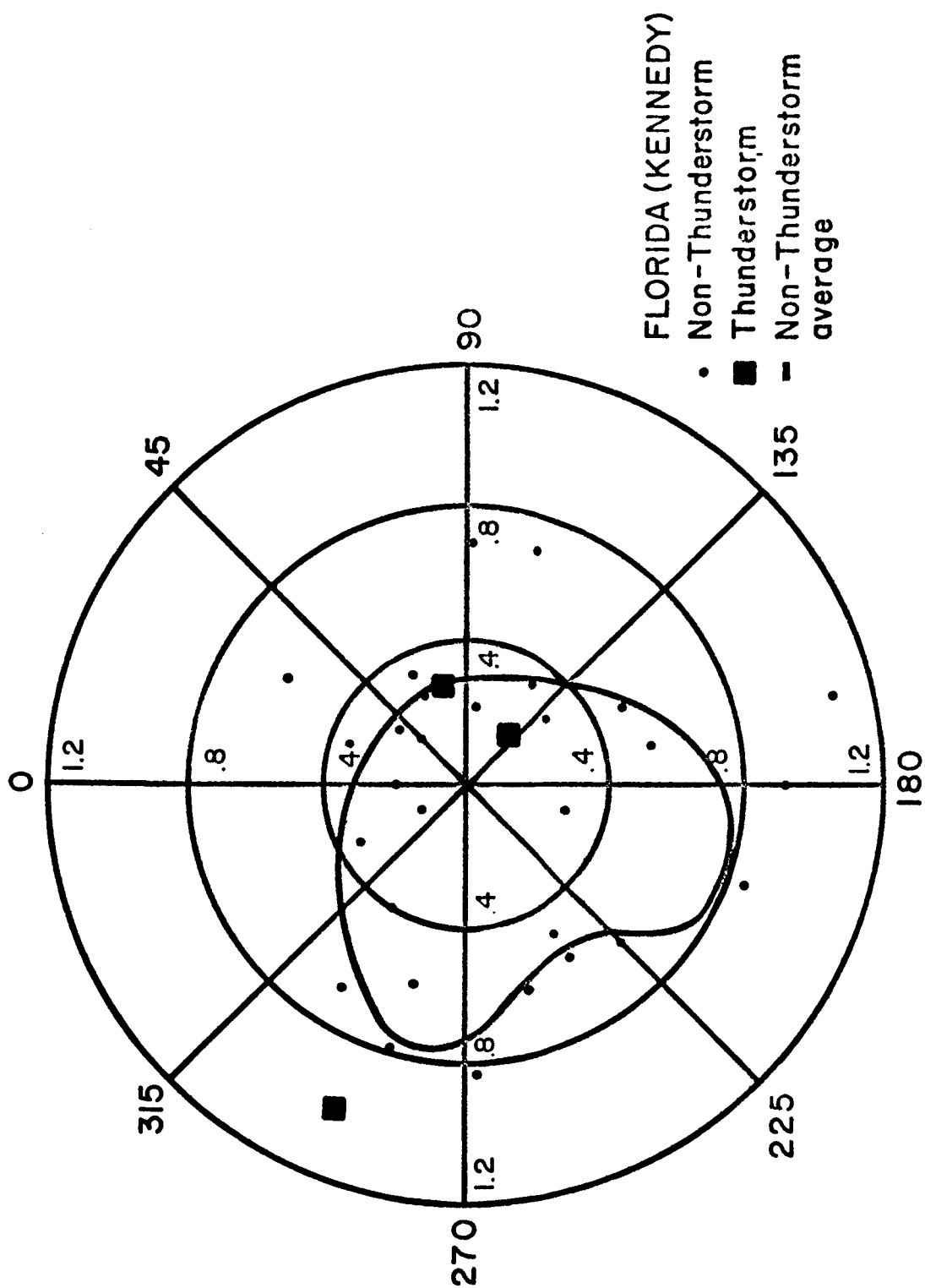


Figure 17. Roughness length, z_0 , as a function of direction at the Cape Kennedy tower (Blackadar et al., 1972).

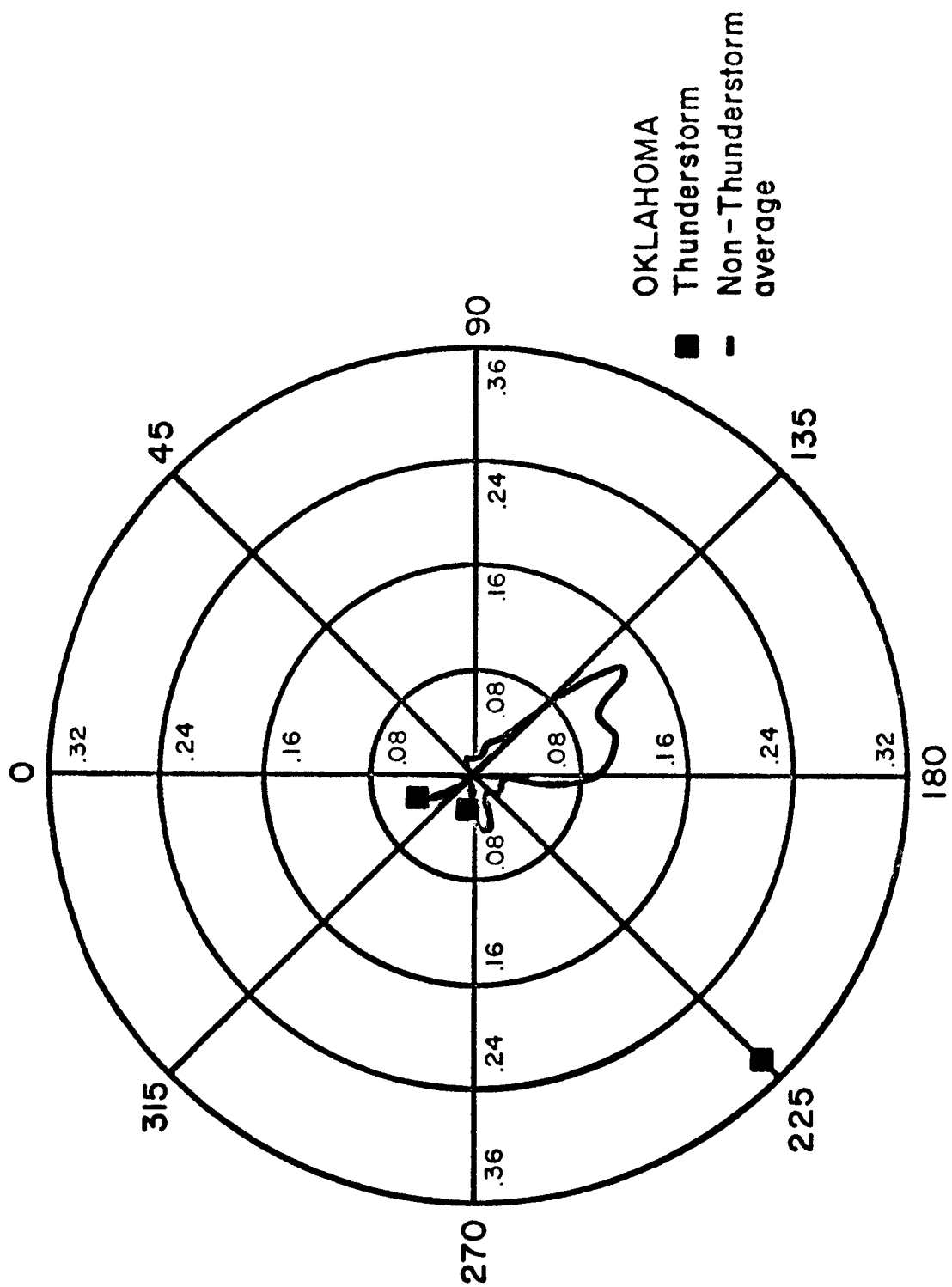


Figure 18. Roughness length, z_0 , as a function of direction at the WKY Oklahoma tower.

At Cape Kennedy (Figure 17), z_0 varies from about 0.3 m for northeasterly winds to about 0.8 m for southwesterly winds. In Oklahoma, the roughness lengths are much smaller than the Cape Kennedy values, ranging from about 0.01 m for easterly winds to about 0.14 m for southeasterly winds.

To compare the values of z_0 that are computed under thunderstorm conditions to the previously determined values, ratios of the wind speed at 90 m to the speed at 18 m were averaged over the gust front for each case. Roughness lengths were then computed from

$$\ln z_0 = \frac{1}{(1 - \frac{V_2}{V_1})} \ln z_2 - \frac{(\frac{V_2}{V_1})}{(1 - \frac{V_2}{V_1})} \ln z_1 \quad (4.3)$$

The average ratios, computed roughness lengths, and average wind direction for each gust front, as well as previously determined roughness lengths, are listed in Table 2. These values of z_0 are also shown in Figures 17 and 18 as a function of wind direction. The agreement between the values of z_0 computed under thunderstorm conditions with the values determined under non-thunderstorm conditions is reasonably good in five out of six cases. This agreement implies that the logarithmic wind law is valid up to about 100 m during the gust front passage and that the differences between the speed ratios in the six gust front cases might be explainable on the basis of different roughness lengths associated with varying terrain and wind directions.

The one Oklahoma case which has a roughness length of .290 m, compared to Sanders and Weber's value of .022 m for the same wind direction,

Table 2. Average wind directions, average ratio of 90 m winds to 18 m winds and corresponding roughness lengths for the six gust fronts. Also shown are previously determined roughness lengths for the listed wind directions.

	GUST FRONT	APPROX. WIND DIRECTION (degrees)	AVERAGE $\frac{V_{90}}{V_{18}}$	THUNDERSTORM z_0 (m)	NON-THUNDERSTORM z_0 (m)
FLORIDA	July 27, 1967	130	1.35	.179	.380
	April 29, 1968	80	1.39	.290	.320
	June 25, 1968	280	1.57	1.079	.750
	April 16, 1969	340	1.27	.042	.053
OKLAHOMA	April 26, 1969	225	1.39	.290	.022
	May 31, 1969	280	1.25	.028	.032

suggests that more data must be analyzed in order to determine the best estimate of roughness length for a particular wind direction at the WKY Tower. The .022 m roughness length is based on a sample of only two cases, and when combined with a value of .290 m found in this study, indicates that the actual roughness length is probably between .22 m and .290 m.

The directional variation of roughness lengths at a site is usually unknown, but by studying the surrounding terrain, a good qualitative estimate of the average roughness length may be made. Such an estimate could then be used to evaluate the ratios of wind speeds at high and low level. Therefore, an average ratio of upper level to lower level winds was determined separately for the three Cape Kennedy and the three Oklahoma cases. Each average ratio corresponds to an average roughness length for each location.

Figures 19-21 indicate the observed time variation of the 90 m wind and the time variation of the 30 m wind profile multiplied by the average ratio V_{90}/V_{30} equal to 1.25 for the three Cape Kennedy cases. Even though z_0 does vary with direction, the use of the average ratio to compute the upper level speed (implying a single average z_0 of 0.4 m) succeeds reasonably well.

A similar comparison of upper level wind (90 m) vs. the lower level wind (7 m) multiplied by the average ratio of the winds at the two levels V_{90}/V_7 is shown in Figures 22-24 for the Oklahoma cases. This ratio was taken as 1.50, implying an average z_0 of .04 m. Again, the agreement is quite good. These results indicate that if

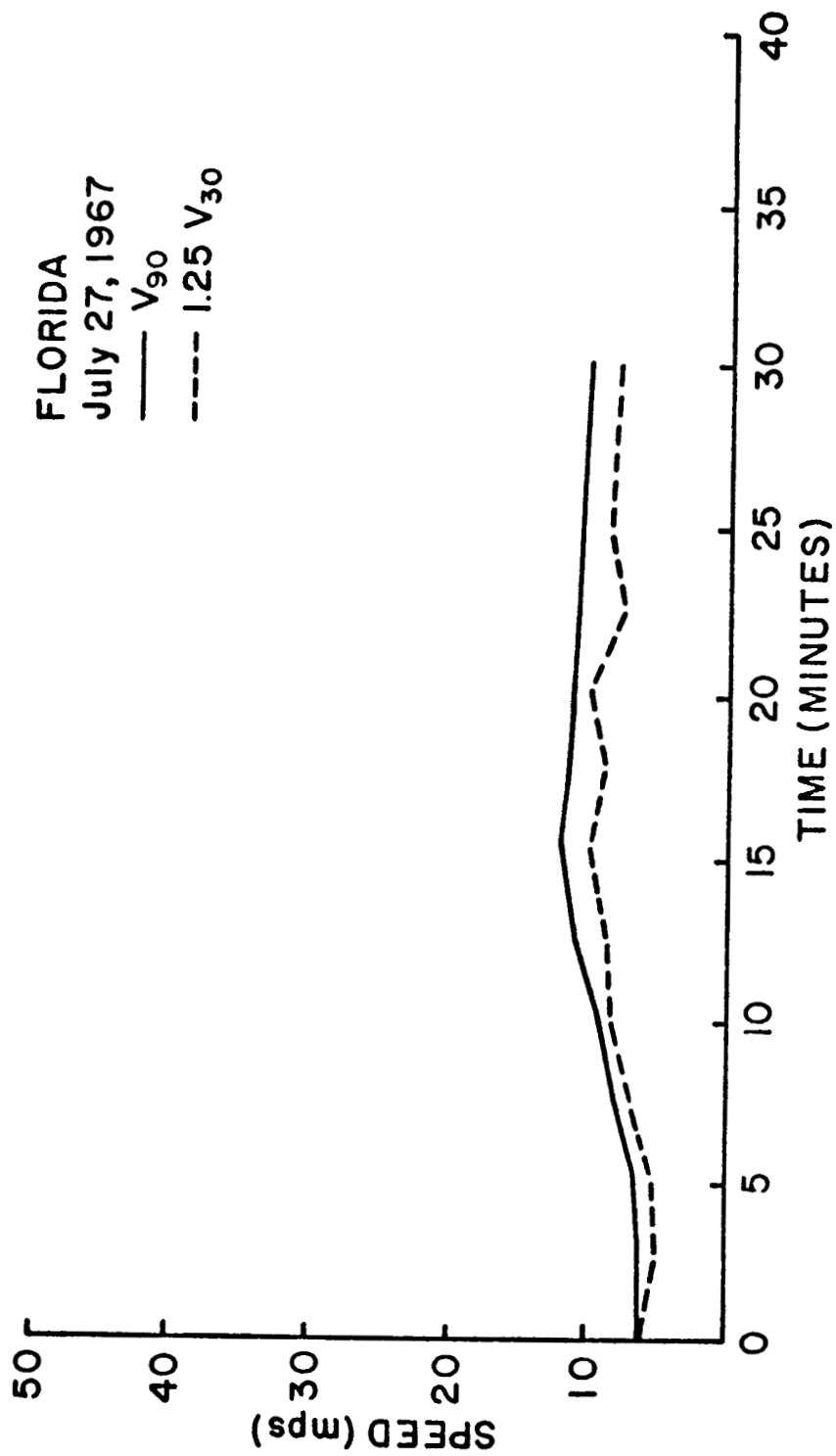


Figure 19. Comparison of observed 90 m wind with the 30 m wind multiplied by the average ratio, V_{90}/V_{30} , for the Florida gust front of July 27, 1967.

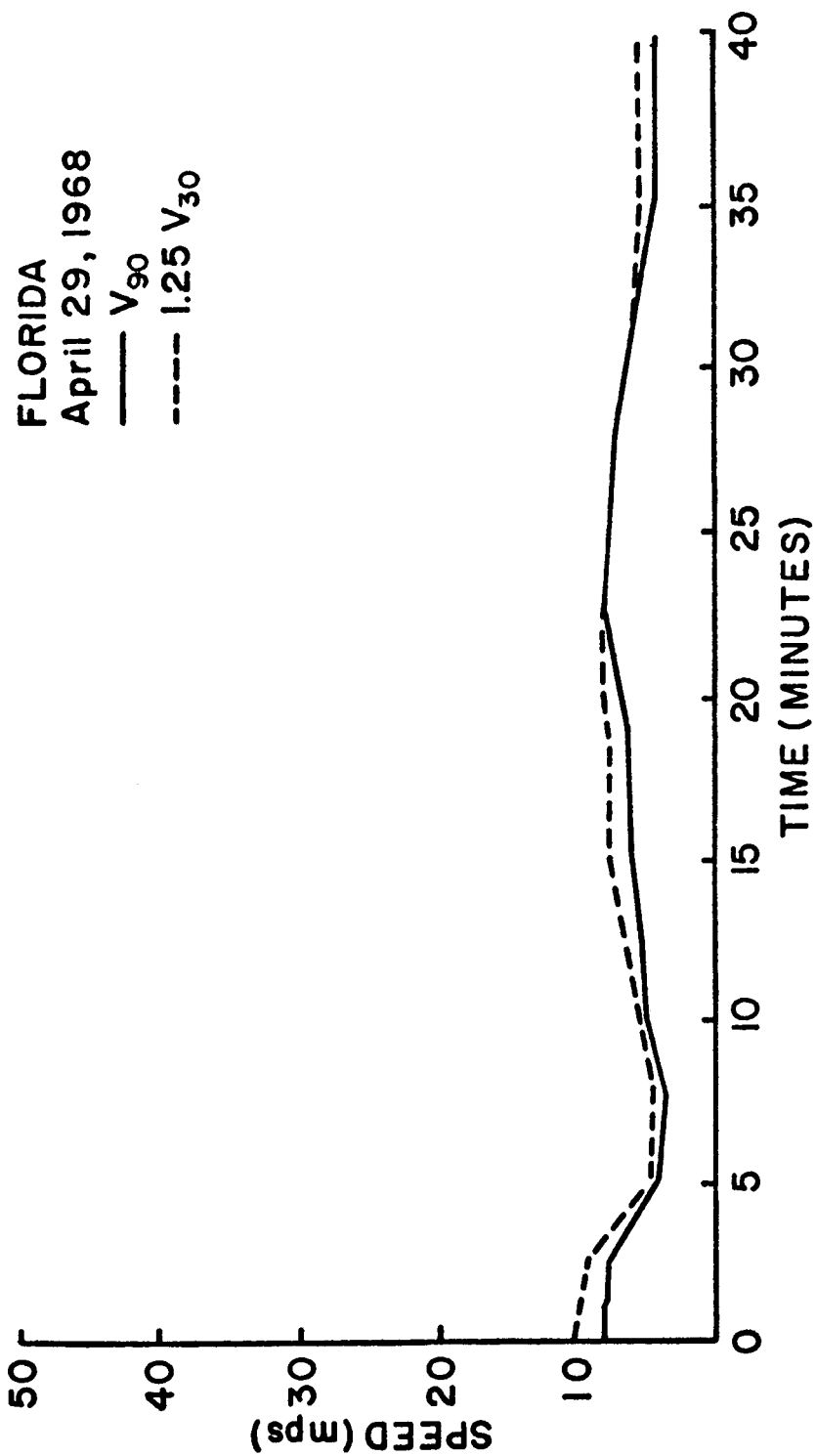


Figure 20. Comparison of observed 90 m wind with the 30 m wind multiplied by the average ratio, V_{90}/V_{30} , for the Florida gust front of April 29, 1968.

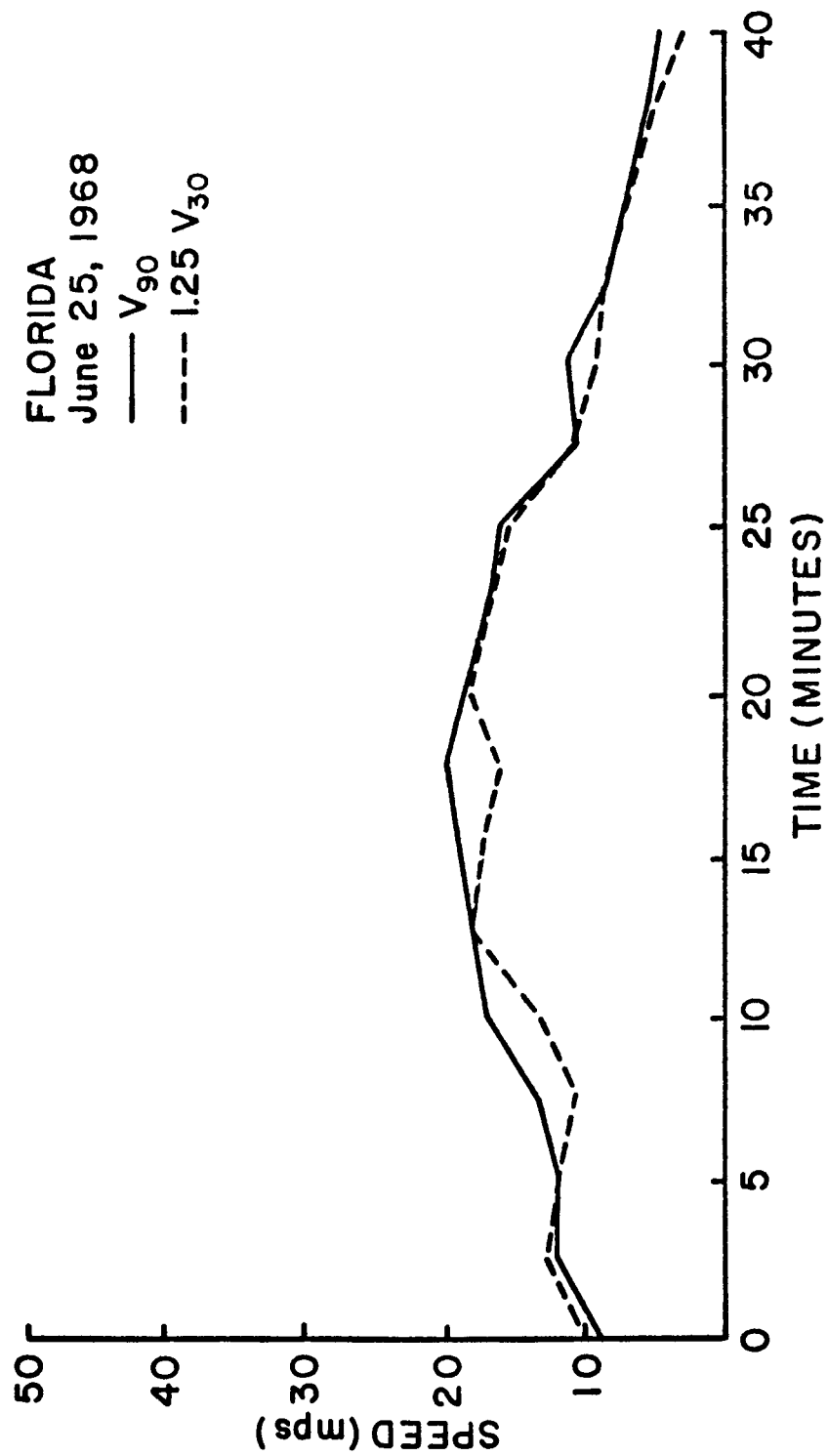


Figure 21. Comparison of observed 90 m wind with the 30 m wind multiplied by the average ratio, V_{90}/V_{30} , for the Florida gust front of June 25, 1968.

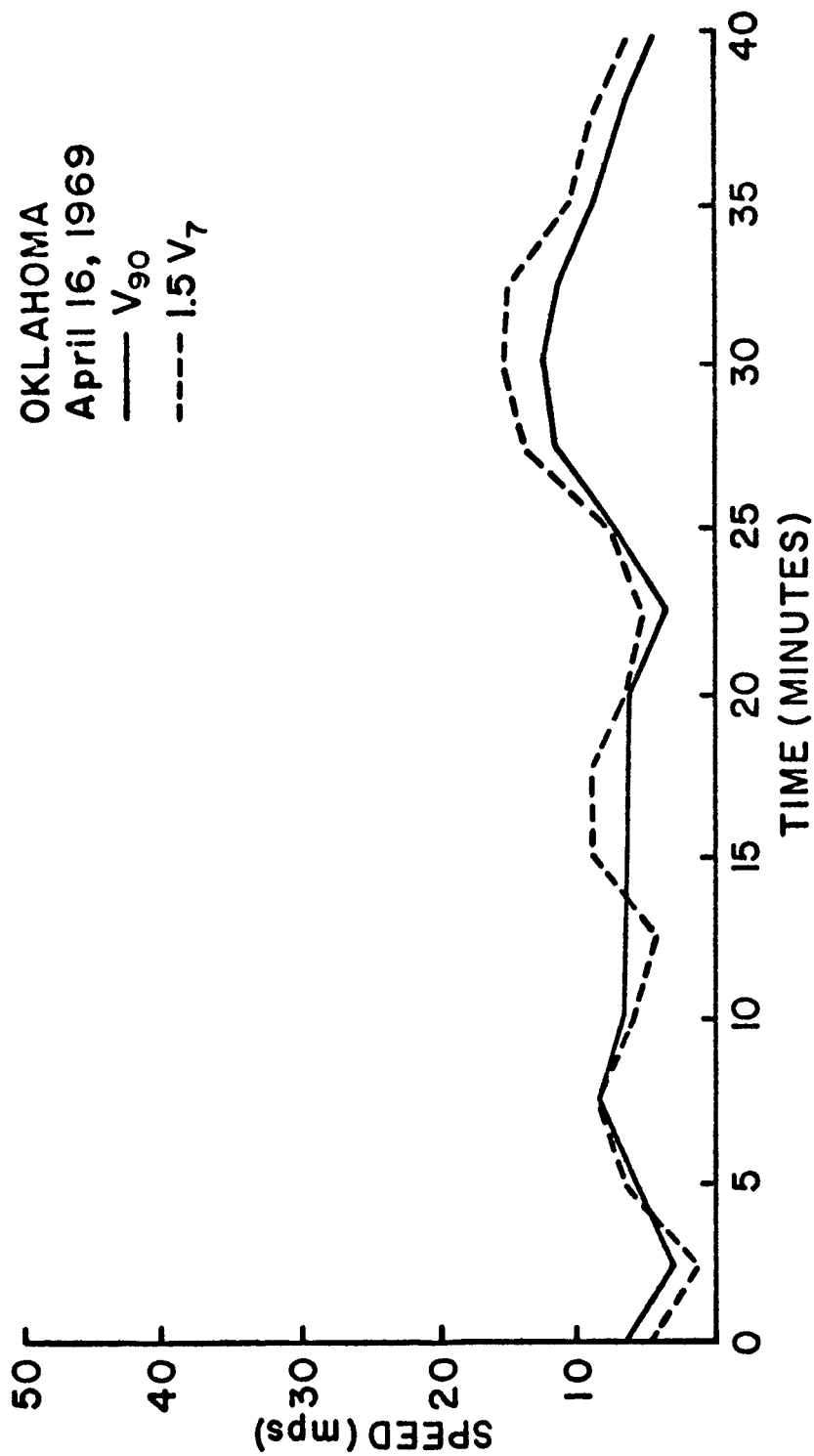


Figure 22. Comparison of observed 90 m wind with the 7 m wind multiplied by the average ratio, V_{90}/V_7 , for the Oklahoma gust front of April 16, 1969.

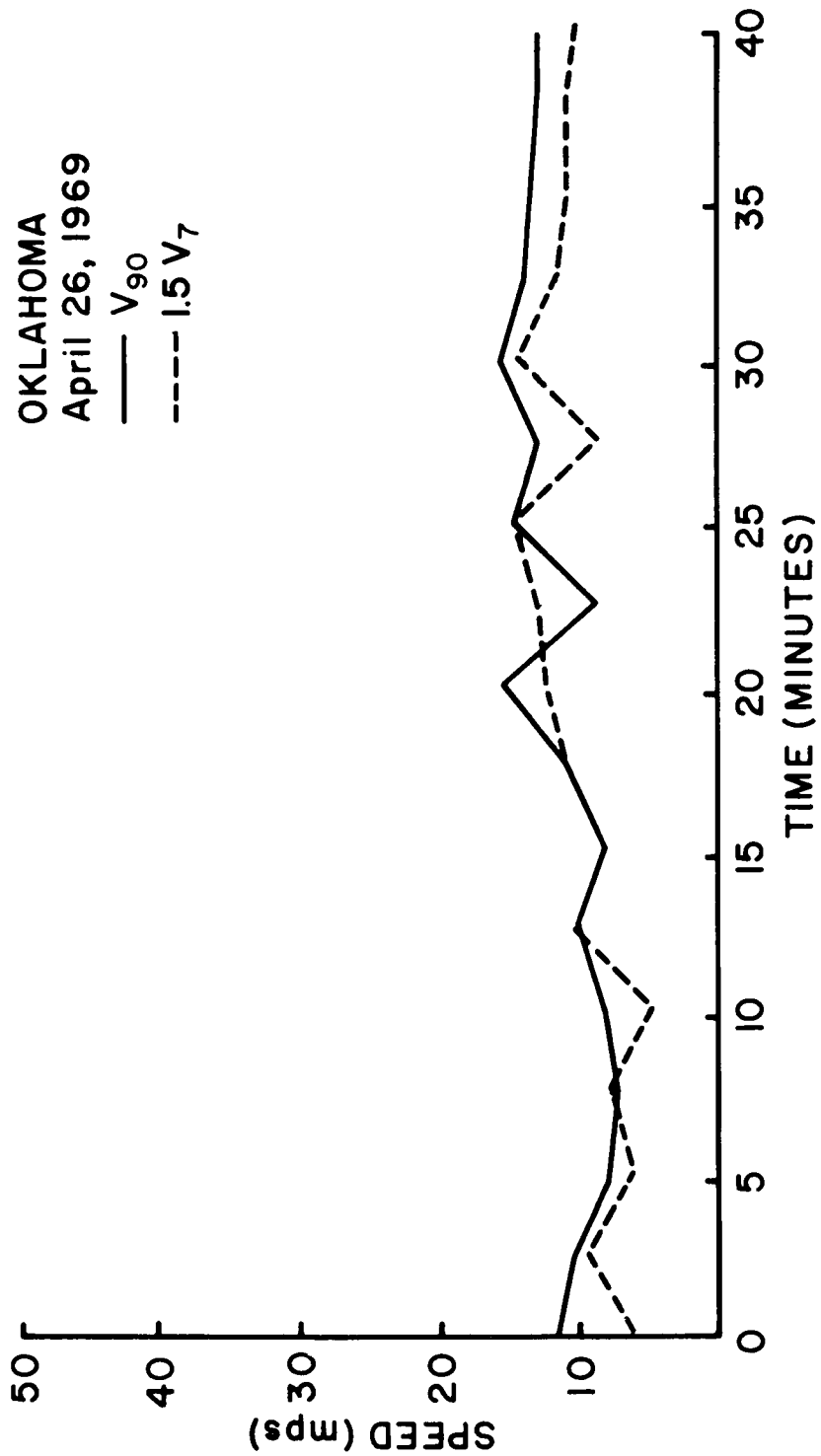


Figure 23. Comparison of observed 90 m wind with the 7 m wind multiplied by the average ratio, V_{90}/V_7 , for the Oklahoma gust front of April 26, 1969.

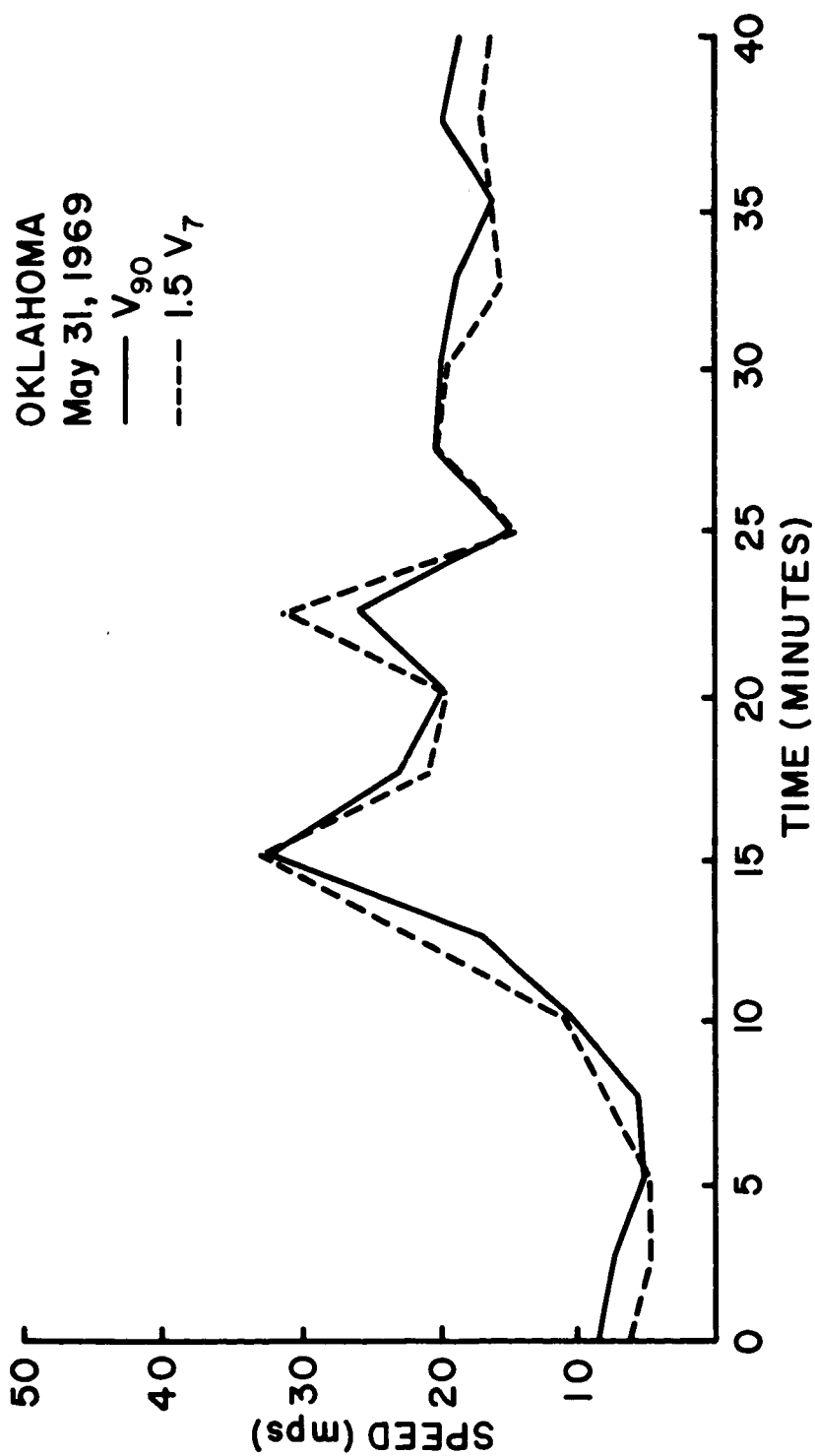


Figure 24. Comparison of observed 90 m wind with the 7 m wind multiplied by the average ratio, V_{90}/V_7 , for the Oklahoma gust front of May 31, 1969.

the time dependent behavior of the wind at one lower level is known, the variation of the wind at the other levels (up to 100 m) may be closely estimated.

4.4 Implications of the Logarithmic Wind Law for the Prediction of the Gust Front Wind Speeds

Because of the validity of the logarithmic wind law up to about 100 m during the passage of a thunderstorm gust front, the winds up to 100 m are related to a lower level wind in a simple way. Although the wind speed structure above 100 m is quite variable from case to case, the shear is much less than that below 100 m. Thus, as a first approximation, the gust front may be modeled by the logarithmic wind law below 100 m and zero shear above 100 m. Therefore, if the local roughness length and the time dependent wind speed at any one level are known, an estimate of the vertical cross section of wind speed can be made.

The key parameters in specifying the wind speed behavior at a single level are the gust length, Δt , and the gust size, ΔV . If these parameters are known, an estimate of the time dependent wind speed profile may be made by assuming some functional form of the wind increase (for example, linear) over the interval Δt .

The implication of the above results is that a crude estimate of the time-dependent, vertical wind speed structure during the passage of a gust front can be made from knowledge of three parameters: 1) the average roughness length, z_0 , which must be estimated for each location; 2) the gust size, ΔV , and; 3) the gust length, Δt .

The next question to be investigated is whether or not the latter two parameters can be statistically inferred from measurable synoptic scale and radar variables to enable short range predictions of the parameters to be made.

5.0 STATISTICAL RELATIONSHIPS OF GUST FRONT PARAMETERS TO RAWINSONDE AND RADAR VARIABLES

5.1 Choice of Independent Variables

The results of the previous sections have indicated that a crude model of the time-dependent vertical variation of the wind speed during the passage of a thunderstorm gust front may be constructed from knowledge of the roughness length z_0 , the gust length, Δt , and peak gust, V_{\max} . It is therefore important to determine whether or not these parameters are statistically related to dynamic and thermodynamic variables that could be obtained from nearby rawinsonde and/or radar observations. For this purpose, rawinsonde, radar, and surface observations for 81 thunderstorm cases were obtained from Tampa, Florida. Tampa was chosen because of the availability of nearby radar and rawinsonde data and also because thunderstorms there should be representative of subtropical thunderstorms.

The variables chosen to serve as predictors for the parameters V_{\max} and Δt included: 1) the dry instability index, I ; 2) maximum cloud height at the time of the peak gust; 3) environmental wind speed at the maximum cloud height; 4) maximum wind speed between 1000 and 500 millibars; 5) the average surface wind speed prior to the gust; 6) cell speed at the time of the maximum gust.

The dry instability index, I , is a measure of the static stability of the atmosphere. Miller (1967) has previously shown that I is a useful predictor of peak gusts for Florida thunderstorms. The maximum cloud

height is indicative of the intensity of convection and should therefore be positively correlated with V_{\max} . Because the downdrafts in cumulonimbus clouds transport upper level momentum to the surface, V_{\max} should be positively correlated with the wind speed at some upper level. Two measures of the upper level wind were tested as predictors; one, the wind at the cloud top level, and the other, the maximum wind speed below 500 millibars.

The average wind speed at the surface prior to the gust was chosen as an independent variable for the regression analysis because it is plausible that this ambient velocity is an additive component of the gust velocity.

5.2 The Variation of Δt Based on a Simple Kinematic Model

The physical variables that determine Δt are more closely dependent upon the structure of the gust front rather than on larger scale variables. A schematic drawing of the thunderstorm and its associated gust front (Figure 25) illustrates some of the variables upon which Δt depends. We assume, based on observations, that the gust front precedes the precipitation echo by a distance, Δr , that depends on the age of the storm.

In general, the gust front is propagating outwardly with a radial velocity V_r , relative to the precipitation cell, which may also be translating with a velocity C . If we assume that the gust length is proportional to the time between the gust front passage and the arrival of the precipitation echo, we may relate Δt to: 1) the perpendicular distance, ℓ , from the station to the track of the storm center; 2) the radius, r , of the precipitation echo; 3) the speed of translation of the

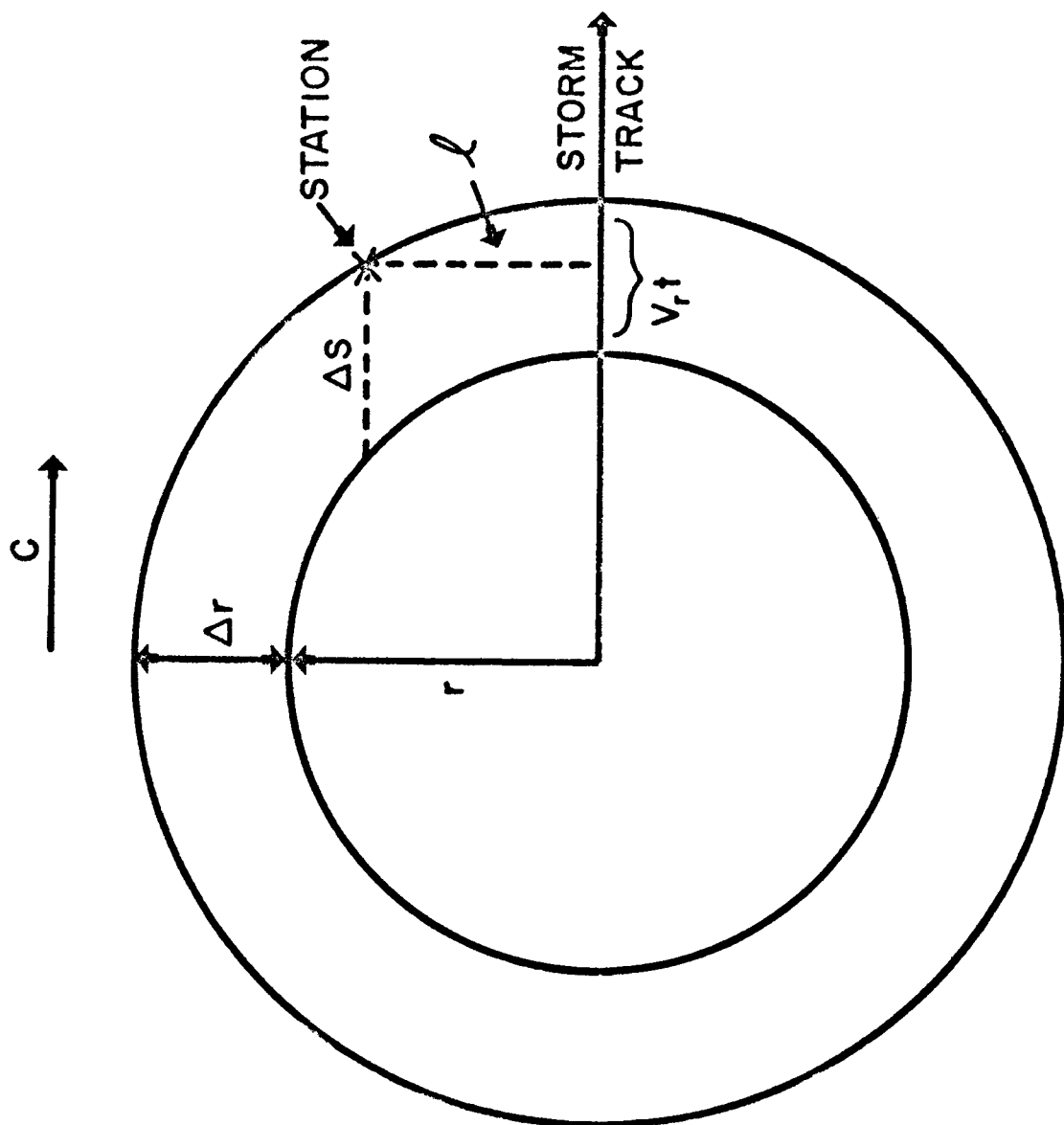


Figure 25. Schematic diagram of gust front.

precipitation cell; 4) the radial velocity of the gust front relative to the precipitation cell; and 5) the age, t , of the gust front, where $t=0$ is defined as the time when $\Delta r=0$. This relationship is

$$\Delta t = \left(\frac{V_r t}{C} \right) \left\{ \frac{\sin \left(90 + \frac{1}{2} \left[\arcsin \left(\frac{\ell}{r} \right) - \arcsin \left(\frac{\ell}{V_r t + r} \right) \right] \right)}{\sin \left(90 - \frac{1}{2} \left[\arcsin \left(\frac{\ell}{r} \right) + \arcsin \left(\frac{\ell}{V_r t + r} \right) \right] \right)} \right\} \quad (5.1)$$

Figure 26 shows the dependence of Δt on the age of the cell and the radial velocity of the gust front. Each curve was determined for a station 800 m from the center of the storm track for a precipitation cell of 1000 m radius translating at 5 mps. The three curves corresponding to different radial velocities indicate that Δt is very sensitive to the radial velocity of the gust front over the gust front lifetime, so that, a slight increase in radial velocity produces a large increase in Δt with time.

The variation of Δt with precipitation cell radius and station distance from the center of the storm track is illustrated in Figure 27. In this calculation the precipitation cell speed, radial velocity of gust front and gust front age were defined by $C=5$ mps, $V_r=2$ mps, and $t=10$ minutes. As shown in Figure 27, Δt does not vary with r at $\ell=0$. Furthermore, Δt is relatively insensitive to the distance of the station from the center of the storm track until that distance exceeds about two-thirds of the cell radius. In each case, Δt increases very rapidly as ℓ approaches the cell radius r . Finally, for a given $\ell \neq 0$, the storms with the smaller

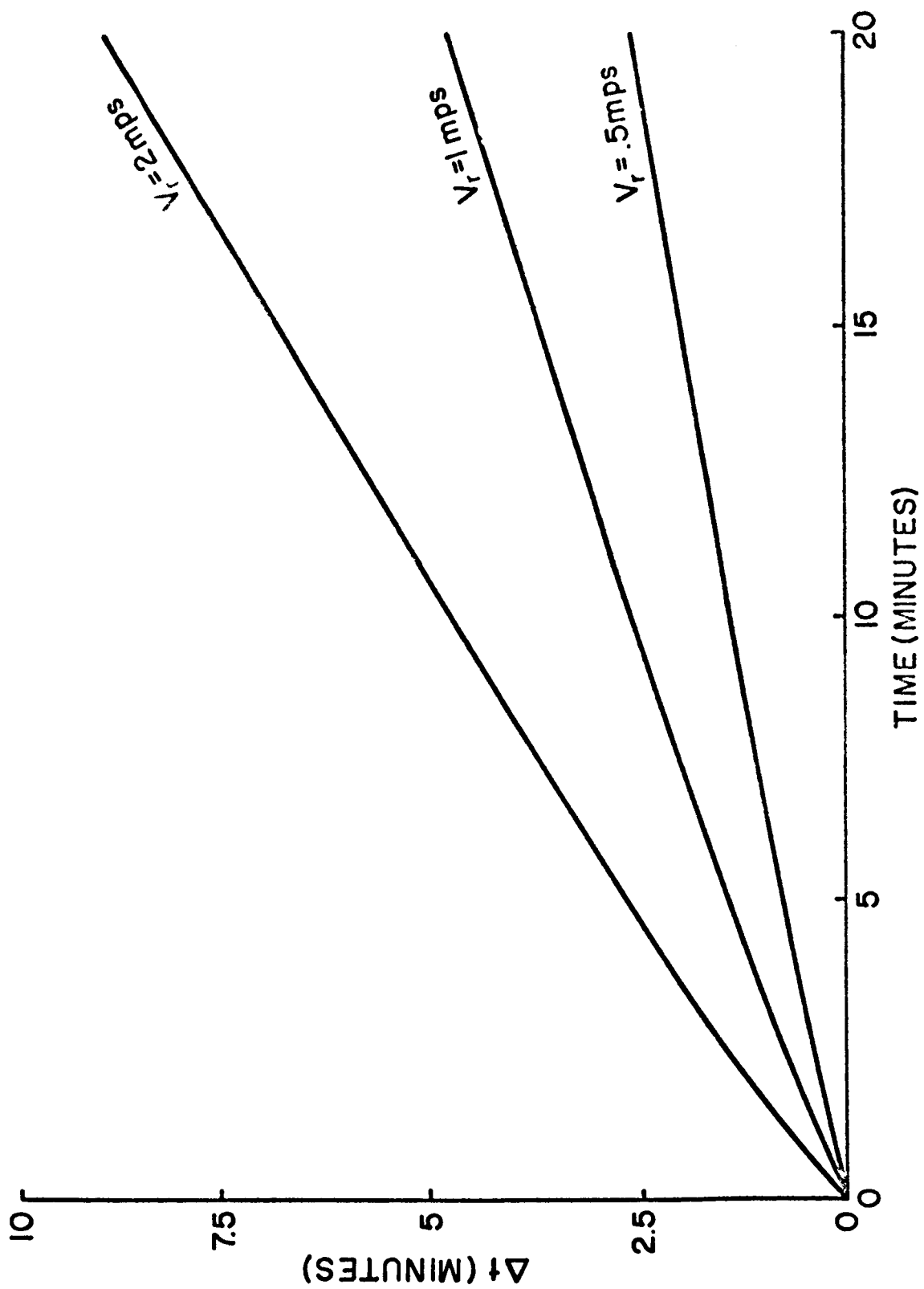


Figure 26. Δt vs. gust front age (Time).

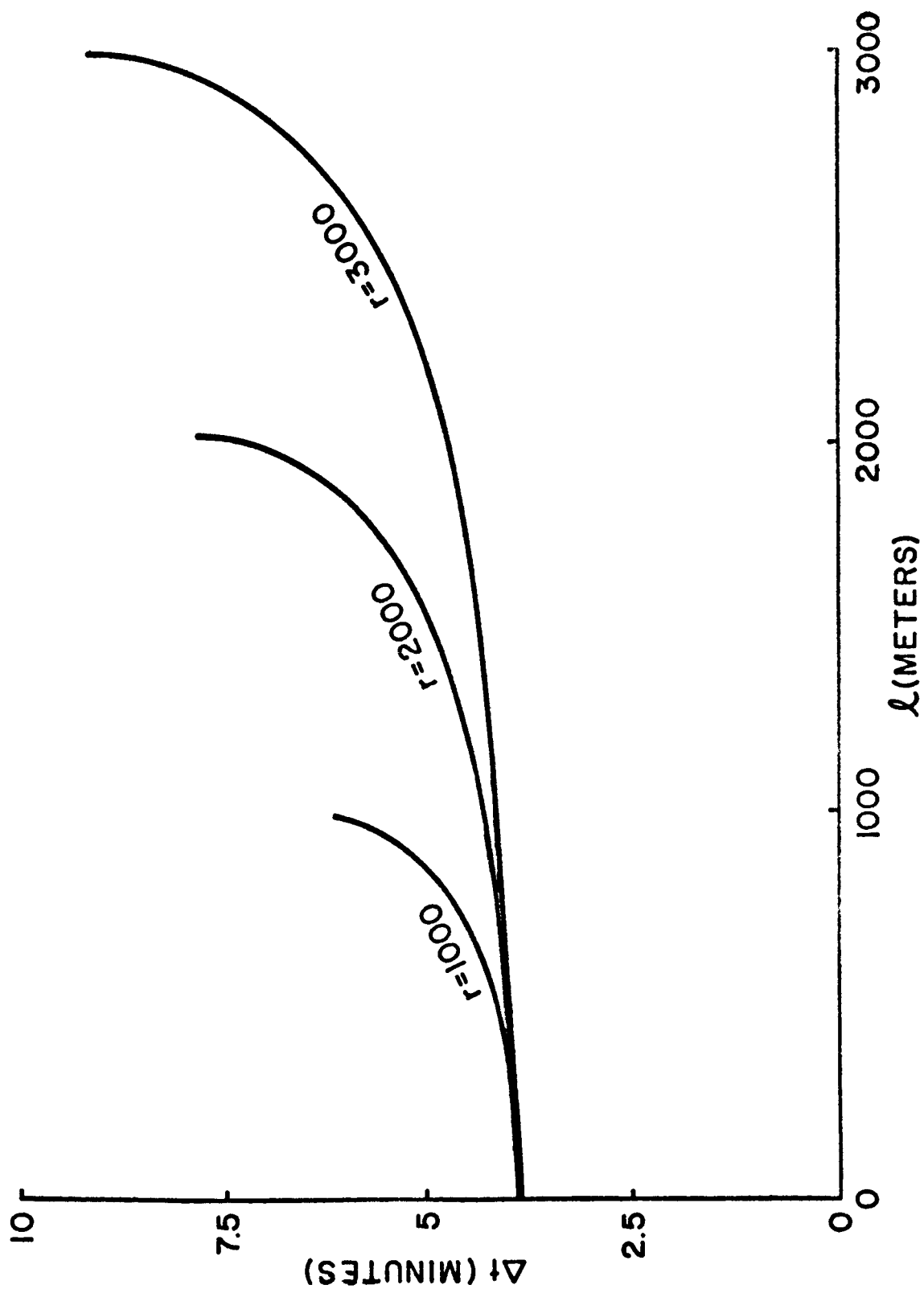


Figure 27. Δt vs. station distance from center of storm track (L).

radii are associated with the largest values of Δt .

In summary, a simple kinematic model yields reasonable values of gust length Δt as a function of the age of the storm, the speed of the storm movement, outward propagation velocity of gust front with respect to the thunderstorm echo, cell radius, and distance of the station from the track of the storm. For a typical range of these parameters, Δt varies from zero to ten minutes.

5.3 Development of Regression Equations

The regression analyses were performed on an IBM 360/67 computer. Means and standard deviations of each variable and correlation coefficients for each possible pair of variables were computed. These means, standard deviations, and correlation coefficients are listed in Table 3.

The first column of Table 3 lists the independent and dependent variables. The second and third columns give the respective means and standard deviations for each variable. The last six columns, when matched with the eight variables in column one, show the correlations between all possible pairs of variables.

As expected, the cell speed is positively correlated ($r=0.37$) with the maximum wind in the 1000-500 millibar layer. A relatively strong correlation (0.32) also exists between the instability index and the average surface wind speed prior to the gust. The higher average wind speeds are associated with the more unstable conditions. The physical basis for this correlation is the increased vertical exchange of momentum under unstable conditions. Under unstable conditions, therefore, high momentum

from aloft is carried downward and low momentum near the surface is transported upward. This reasoning also explains the significant negative correlation of -0.27 between the instability index and the wind speed at cloud tops.

The second part of the analysis was a step-up multiple linear regression procedure, in which number of multiple linear regression equations were computed. These equations are obtained by adding or deleting one variable at a time, giving regression equations at intermediate steps

$$\begin{aligned}
 \hat{y}_1 &= b_0^0 + b_1^0 x_1 \\
 \hat{y}_2 &= b_0^1 + b_1^1 x_1 + b_2^1 x_2 \\
 \hat{y}_3 &= b_0^2 + b_1^2 x_1 + b_2^2 x_2 + b_3^2 x_3 \\
 &\vdots \\
 \hat{y}_n &= b_0^{n-1} + b_1^{n-1} x_1 + b_2^{n-1} x_2 + \dots + b_n^{n-1} x_n
 \end{aligned} \tag{5.2}$$

where the \hat{y}_i are the best estimates in a least squares sense of the independent variable (the predictand) and the x_i are the various predictors.

The coefficients, b_i , in equation (5.2) are determined by minimizing

$$E = \sum_{i=1}^{81} (y - \hat{y}_i)^2 \tag{5.3}$$

Table 3. Means and standard deviations for each variable and correlation coefficient for each possible pair of variables for the 81 thunderstorm cases from Tampa, Florida.

Variable	Mean	Std. Dev.	\bar{V}_s	Cell Spd.	I	$V_{1000-500}$	Cld. Hgt.	$V_{Cld. Hgt.}$
\bar{V}_s (mps)	3.8	1.2						
Cell Spd. (mps)	5.8	3.4	-0.01					
I (°C)	10.2	4.7	0.32	-0.19				
$V_{1000-500}$ (mps)	9.0	3.2	0.06	0.37	-0.11			
Cld. Hgt. (ft)	37600	7400	-0.17	0.02	-0.20	0.04		
$V_{Cld. Hgt.}$ (mps)	9.8	5.3	-0.07	0.07	-0.27	0.11	0.16	
V_{max} (mps)	8.8	2.8	0.53	0.05	0.41	0.15	-0.02	0.05
Δt (min)	5.4	4.5	-0.16	0.01	0.05	-0.05	-0.06	0.02

the sums of squares of the deviations of the observed value, y_i from the predicted value \hat{y}_i . In determining the intermediate regression equations, variables were added in the order which yielded the greatest reduction in the error E. If the variance reduction associated with a given independent variable is insignificant at a specified level (2.5 F level), the variable is not included in the regression. Therefore, the final equation contains only those variables that explain important portions of the variance. A more detailed discussion of the step-up regression procedure is given by Efroymson (1967).

5.4 Discussion of Regression Equation

The results from the 81 Tampa thunderstorm cases showed that no independent variables were significantly correlated with the parameter Δt and no regression equation was formed. This result indicates that Δt cannot be estimated from the larger scale rawinsonde and radar parameters studied here. As discussed in section 5.2, Δt is a strong function of variations in cell radius, cell age, motion of the cell, and position of the station with respect to the center of the storm track. Since these variables were unknown, it is not surprising that Δt was uncorrelated with any of the independent variables.

In the analysis for the peak wind gust, two independent variables, the surface wind speed prior to the gust and the dry instability index, were correlated relatively strong with the peak gust. Figure 28 shows a scatter diagram of the gust speed vs. the average surface wind speed.

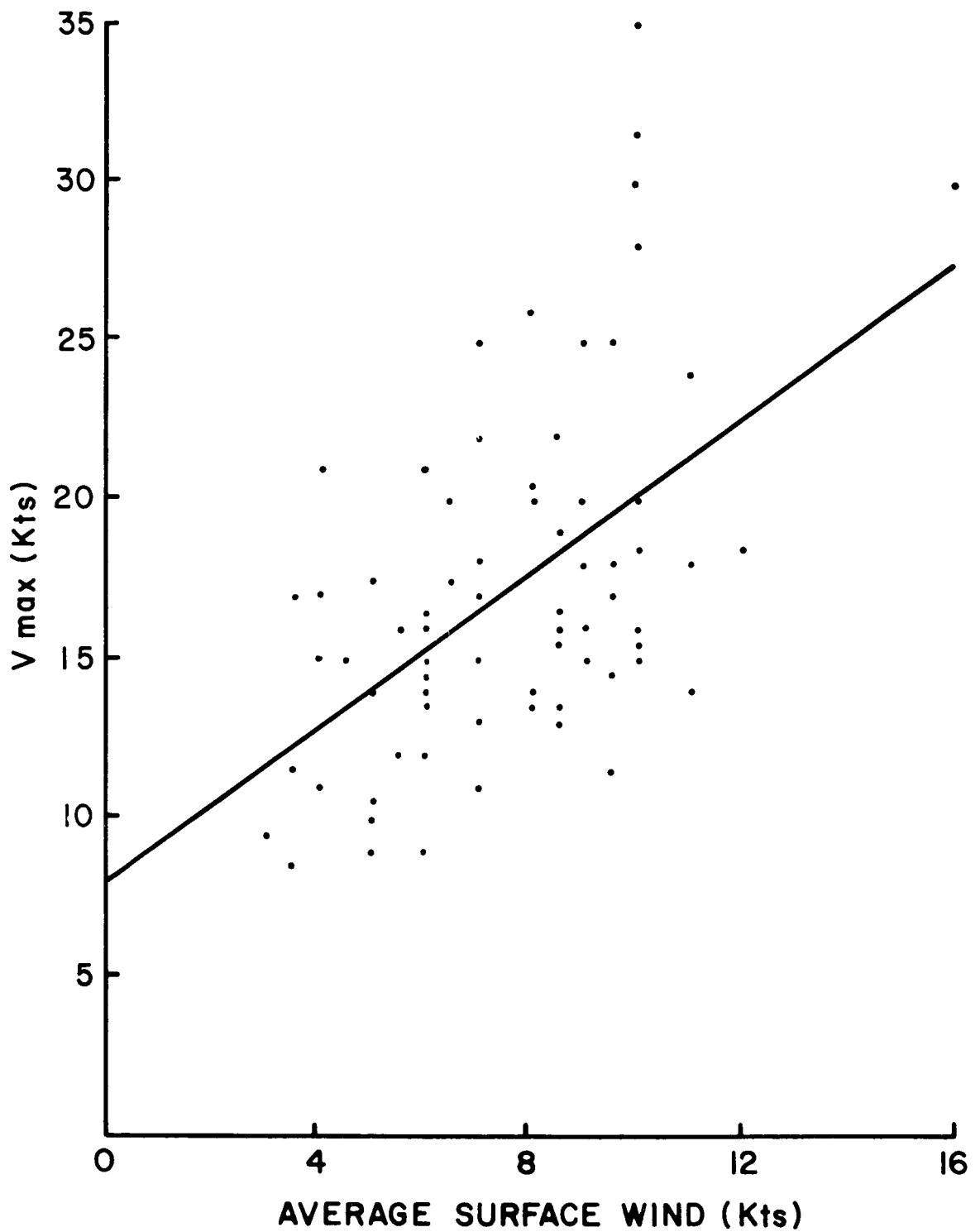


Figure 28. Scatter diagram with line of best fit of the speed maximum vs. the average speed before the gust front.

The line of best fit is also shown. Figure 29 shows the gust speed as a function of the instability index, with the line of best fit also shown. Both figures exhibit considerable scatter.

The regression equation relating the peak gust (in mps) to the average surface wind and the instability index is

$$V_{\max} = 3.2 + 1.02 \bar{V}_s + .158 I \quad (5.4)$$

where \bar{V}_s is expressed in mps and I is expressed in degrees Celsius. However, these two independent variables explained only thirty-four percent of the variance of peak gusts, and therefore are of only limited use in prediction.

The small percentage of explained variance for V_{\max} is somewhat disappointing, but not unexpected in view of the complexity of the unsteady, three-dimensional thunderstorm circulation. There are several possible explanations why so little variance was explained. First, there may be additional important independent variables that were not tested. The possibility of finding additional significant variables is considered unlikely because environmental variables that are known to be important in thunderstorm development (static stability and vertical wind shear) have already been included.

A second and more plausible explanation is that the rawinsonde parameters were not representative of the environment in the immediate vicinity of the thunderstorm cell. Many of the rawinsonde data were six hours earlier or later than the thunderstorm, during which time the

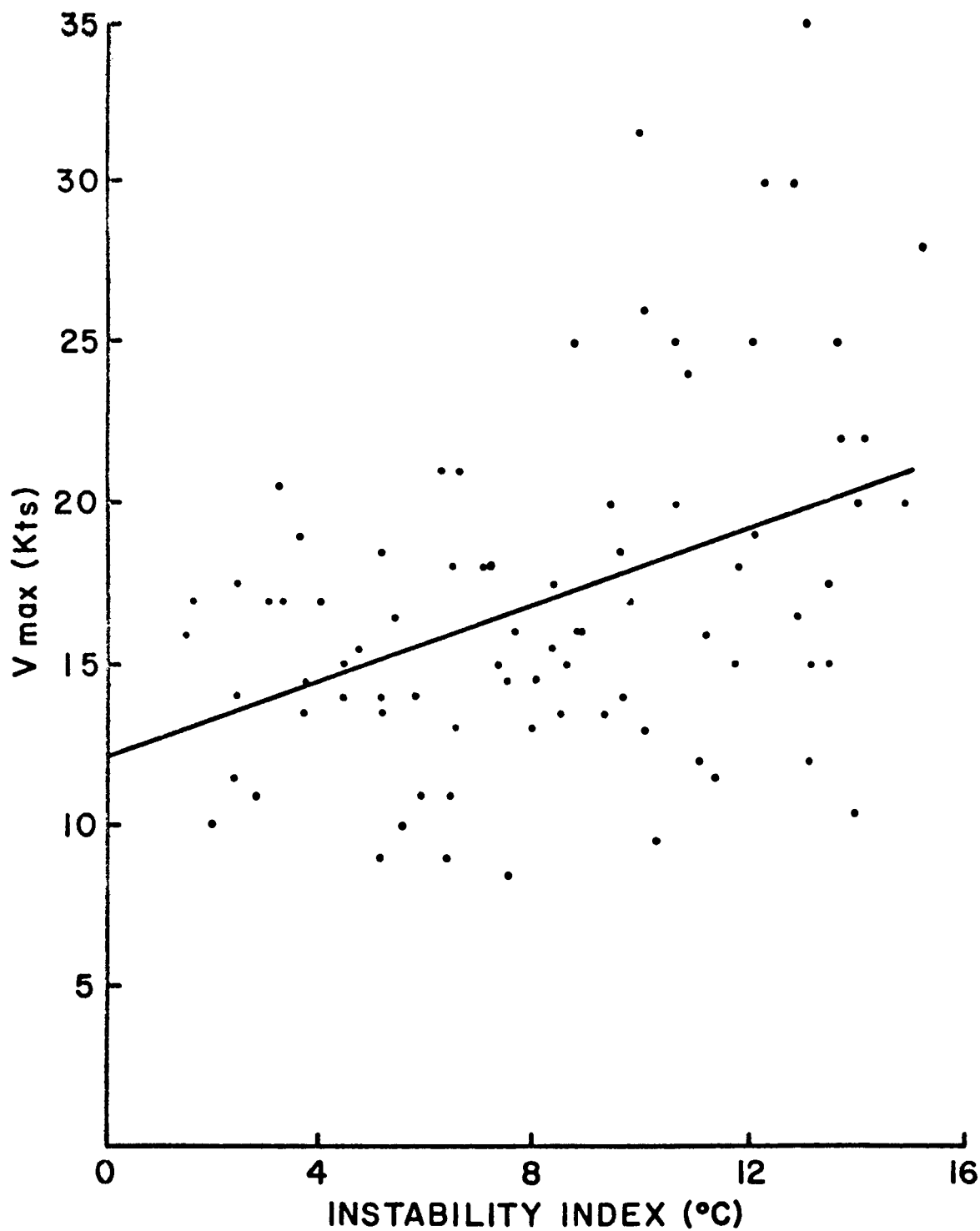


Figure 29. Scatter diagram with line of best fit of the speed maximum vs. the instability index.

environmental variables could have changed appreciably. It is probable that simultaneous soundings in the immediate vicinity of the thunderstorms would provide further reduction of the scatter.

A third possibility is that dependent variable V_{\max} is a point estimate and may not be representative of the average peak gust associated with the thunderstorm. In the three-dimensional gust front structure, wide variation with respect to age of the gust front, and position with respect to the thunderstorm center may be expected. Thus, to expect any real reduction in scatter, one would have to stratify the data according to these two parameters.

REFERENCES

- Aerospace Sciences Review, "Thunderstorm Wind-Gust Forecasts," April 1966, 13.
- Blackadar, A. K., J. A. Dutton, H. A. Panofsky, and A. Chaplin, 1972: Investigation of turbulent wind field below 150 m altitude at the Eastern Test Range, Final Report in Preparation, NASA Contactor Report CR-1410.
- Brancata, G. N., 1942: The meteorological behavior and characteristics of thunderstorms, USWB, April 1942.
- Charba, J. P., 1972: Gravity current model applied to analysis of squall-line gust front. The University of Oklahoma, Ph.D. Dissertation, 1972, 100 pp.
- Colmer, M. J., 1971: On the character of thunderstorm gust-fronts. Royal Aircraft Est., Bedford, England, Eng., 11 pp.
- Efroymson, M. A., 1971: "Multiple Regression Analysis." Mathematical Methods for Digital Computers, edited by A. Ralston and H. S. Wolfe, New York: John Wiley and Sons, 1965.
- Fawbush, Lt. Col. E. J. U.S.A.F. and Maj. R. C. Miller U.S.A.F., 1954: A basis for forecasting peak wind gusts in non-frontal thunderstorms. Bull. Amer. Meteor. Soc. 35, 14-19.
- Feteris, P. J., 1965: Statistical studies on thunderstorm situations in the Netherlands. J. Appl. Meteor., 4, 178-185.
- Foster, D. S., 1958: Thunderstorm gusts compared with computed downdraft speeds. Mon. Wea. Rev., March 1958, 91-94.
- Hiser, H. W., H. V. Sennand C. L. Courtright, 1970: Identification of damaging surface winds in tropical thunderstorms utilizing incoherent weather radar and meteorological observations. Final Report, University of Miami, Rosentiel School of Marine and Atmospheric Reasearch, AFCRL 70-0542, 1970, 25 pp.
- Kaufman, J. W. and L. F. Keene, 1968: NASA's 150mm meteorological tower located at the Kennedy Space Center, Florida. NASA Tech. Memo. TMX-53699, 22 pp.
- Miller, R. C., 1967: Forecasting thunderstorm-produced surface wind gusts in Southeast Asia. Unpublished Report: February 1967, 1-13.

REFERENCES (Continued)

- Sanders, L. D. and A. H. Weber, 1970: Evaluation of roughness lengths at the NSSL-WKY meteorological tower. ERLTM-NSSL 47, 24 pp.
- Sherlock, R. J. and M. B. Stout, 1937: Wind structure in winter storms. J. Aeronautical Sciences, 5, 53-61.
- Simpson, J. E., 1969: A comparison between laboratory and atmospheric density currents. Quart. J. R. Meteor. Soc., 95, 758-765.